JOC The Journal of Organic Chemistry

Article

pubs.acs.org/joc

# Design, Preparation, and Study of Catalytic Gated Baskets

Bao-Yu Wang, Teodora Žujović, Daniel A. Turner, Christopher M. Hadad, and Jovica D. Badjić*

Department of Chemistry, The Ohio State University, Columbus, Ohio 43210, United States

Supporting Information

**ABSTRACT:** We report a diastereoselective synthetic method to obtain a family of catalytic molecular baskets containing a spacious cavity (~570 Å$^3$). These supramolecular catalysts were envisioned, via the process of gating, to control the access of substrates to the embedded catalytic center and thereby modulate the outcome of chemical reactions. In particular, gated basket **1** comprises a porphyrin "floor" fused to four phthalimide "side walls" each carrying a revolving aromatic "gate". With the assistance of $^1$H NMR and UV−vis spectroscopy, we demonstrated that the small 1-methylimidazole guest (**12**, 94 Å$^3$) would coordinate to the interior while the larger 1,5-diadamantylimidazole guest (**14**, 361 Å$^3$) is relegated to the exterior of basket Zn(II)−**1**. Subsequently, we examined the epoxidation of differently sized and shaped alkenes **18**−**21** with catalytic baskets **12**$_{in}$−Mn(III)−**1** and **14**$_{out}$−Mn(III)−**1** in the presence of the sacrificial oxidant iodosylarene. The epoxidation of *cis*-stilbene occurred in the cavity of **14**$_{out}$−Mn(III)−**1** and at the outer face of **12**$_{in}$−Mn(III)−**1** with the stereoselectivity of the two transformations being somewhat different. Importantly, catalytic basket **14**$_{out}$−Mn(III)−**1** was capable of kinetically resolving an equimolar mixture of *cis*-2-octene **20** and *cis*-cyclooctene **21** via promotion of the transformation in its cavity.

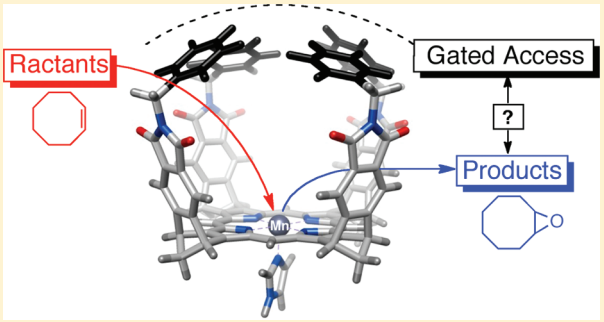


## INTRODUCTION

Ever since Cram's seminal paper[1] about the prospect of molecular encapsulation, many covalent[2−4] and self-assembled[5,6] capsules have been made[7] and demonstrated to entrap smaller compounds having complementary size, shape, and functionality. Indeed, the isolation of a guest in the interior of a host provides the entrapped compound with a unique environment sometimes referred to as "a new state of matter".[8] By way of encapsulation, one can thus modulate the persistence of reactive intermediates[9,10] and even change the course/rate of chemical reactions[11−13] or conformational changes.[14] The mechanism by which the entrapment occurs[15] is typically a function of the host's structure, and in accord with one of the following mechanistic scenarios: slippage, dissociation, or gating.[15] In particular, gating[15,16] comprises a conformational change in the host that regulates the rate (e.g., the constrictive binding energy $\Delta G^{\ddagger}$)[17] by which guests enter or depart the host. Enzymes use gating for controlling the selectivity of catalytic reactions,[18] while ion/molecular channels employ gating for regulating the trafficking of ions across cell membranes.[19] *This study poses a question about the relationship between the gating of reactants and its effect on the outcome of a chemical* reaction *occurring inside a gated catalyst.* In particular, we would like to understand if modulating (1) the residence time of encapsulated reactant(s) and/or (2) its access to such a gated catalyst[20,21] has any effect on the reaction's yield, stereoselectivity, and/or product distribution.

We[22−26] and others[27−32] have, during the past decade, explored gated hosts and their mechanisms of operation. Importantly, there have been no studies about gated catalysis, but investigations on the effect of the catalyst's dynamics on the reaction's outcome are emerging.[33−36] Accordingly, the present work focuses on the design, synthesis, and optimization of the catalytic behavior of a new family of gated baskets (Figure 1). These compounds comprise a porphyrin "floor" surrounded with four phthalimide-based "walls" for forming a semirigid platform (Figure 1A).[37] The aromatic "gates" are placed at the top of the platform to, via $CH_2$ "hinge" groups, revolve about the basket's entrance/exit and thereby regulate the access of guests to the catalytic center (Mn(III)) embedded in the cavity (Figure 1A).

On the basis of our previous study,[39] we first developed a reliable synthetic method for the preparation of catalytic molecular baskets (Figure 1). Next, we used $^1$H NMR and UV−vis spectroscopic methods for quantifying the axial coordination of differently sized imidazoles to zinc(II)- and manganese(III)-metalated baskets. Finally, we examined the epoxidation of alkenes[40−44] inside and outside the cavity (~570 Å$^3$, Figure 1B) of Mn(III)-containing baskets. In particular, the oxygen atom transfer (OAT) reaction was promoted with monomeric and soluble iodosylarene (*t*-Bu$SO_2$PhIO).[45,46] Consistent with prior work,[47−49] this sacrificial terminal oxidant converted the resting state Mn(III) supramolecular catalyst into an elusive Mn(V)=O species that further transferred the oxygen atom to entrapped alkenes (Figure 1A). *Importantly, the results of our catalytic studies suggest that gated baskets are capable of promoting the epoxidation of differently sized-alkenes in their*

**Received:** December 6, 2011
**Published:** February 3, 2012

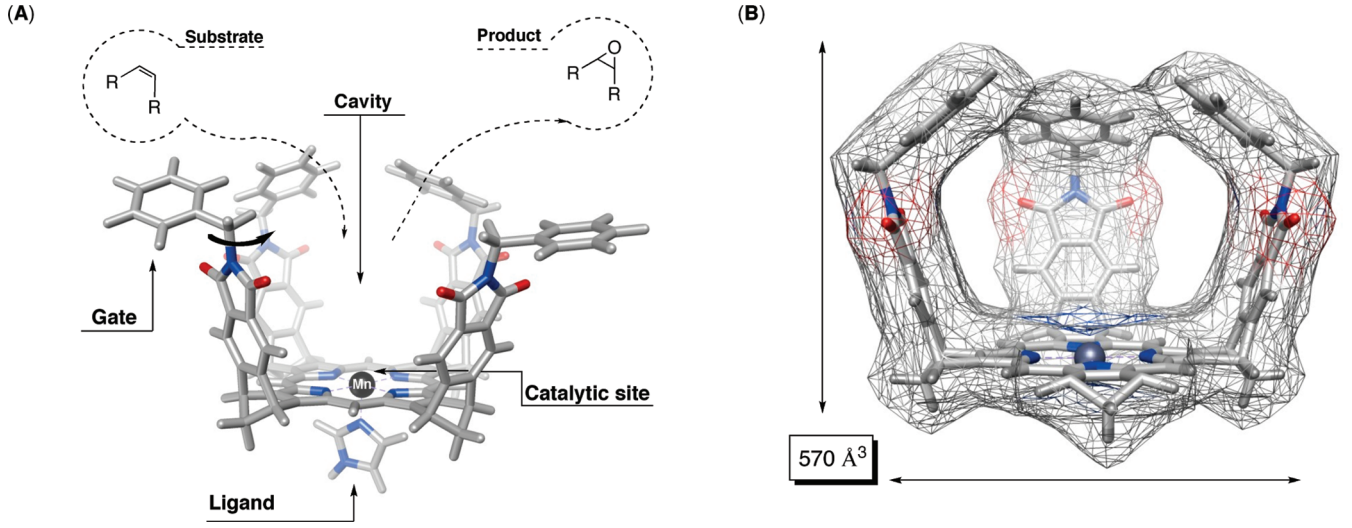


**Figure 1.** (A) Catalytic gated baskets comprise a porphyrin "floor", phthalimide "walls", and aromatic "gates". (B) Inner volume of the catalytic basket, with four gates pointing toward the cavity, was estimated to be 570 Å$^3$;[38] note that the right-hand illustration represents a computed van der Waals surface of the basket with the front side omitted for clarity.

**Scheme 1. Synthetic Methodology for Obtaining *Enantiopure* Pyrromethanecarbinol 10**

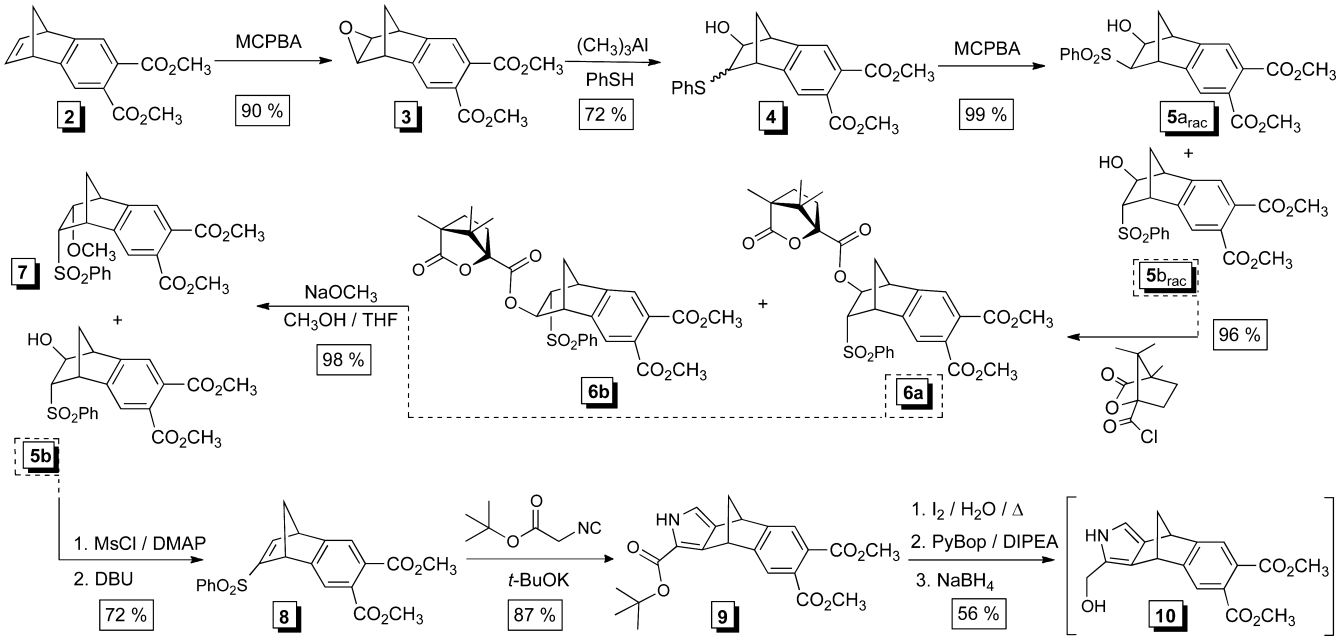


*interior*. The stereoselectivity and rates of these reactions appear to be a function of the size/shape of various alkene substrates.

## RESULTS AND DISCUSSION

**Synthetic Hypotheses.** We recently developed a diastereoselective synthetic method for obtaining cup-shaped porphyrins akin to gated molecular basket in Figure 1.[39] In particular, we showed that *enantiopure* pyrromethanecarbinol, akin to **10** (Scheme 1), would undergo a stereoselective oligomerization in the presence of a Brönsted acid, such as *p*-TsOH, to give a sole porphyrin product with four bicyclic rings pointing to the same direction in space (Scheme 2). The acid-catalyzed condensation was under kinetic control as longer reaction times and higher concentrations of the acid led to the formation of other diastereomeric porphyrins.[39] In accord with such findings, the synthetic strategy for obtaining gated basket **1** (Scheme 2) was based on the notion that compound **10** would undergo a diastereoselective head-to-tail tetramerization and, upon oxidation, give rise to porphyrin derivative **11** (Scheme 2). In addition, we surmised that octaester **11** could easily be transformed into gated basket **1** using a previously described methodology.[50]

**Synthesis.** Benzonorbornadiene derivative **2** was made in multigram quantities following a published procedure.[51] The epoxidation of **2** with *m*-CPBA occurred with exclusive transfer of the oxygen atom to the *exo* side of the norbornene; 2D-NMR NOESY investigation[52] of epoxide **3** revealed $^1$H−$^1$H correlations implying the *exo* position of the epoxide functionality. Compound **3** was further subjected to ring-opening with thiophenol in the presence of Lewis acid $(CH_3)_3Al$[53] (Scheme 1). Interestingly, in this reaction the nucleophile attacked both the *exo* and *endo* sides of **3** to give **4**;


dx.doi.org/10.1021/jo202443j | J. Org. Chem. 2012, 77, 2675−2688

**Scheme 2. Diastereoselective Oligomerization of 10 (5.0 mM) Completed in $CHCl_3$ with *p*-TsOH (0.395 mM) at Room Temperature**[a]

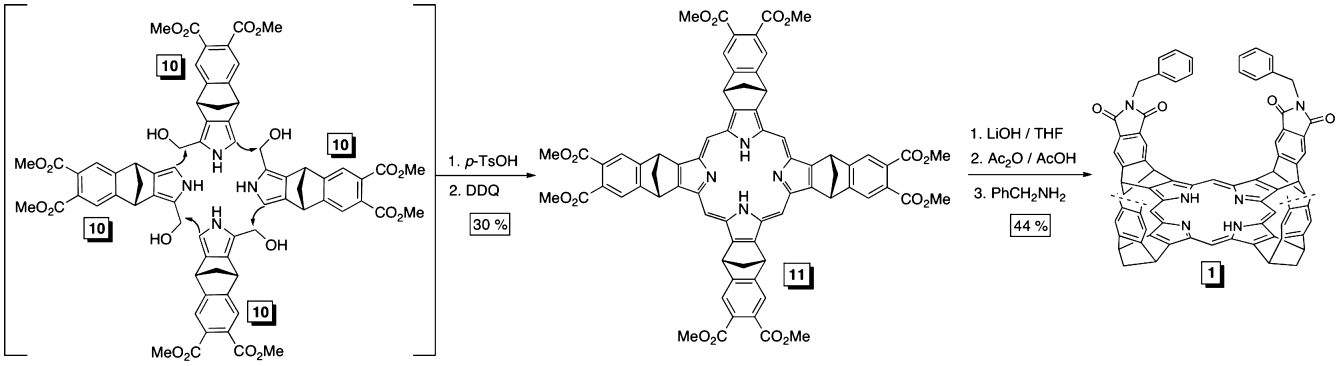


[a]For the chemical structure of **1**, see Figure 2A.

note that **4** was obtained as a mixture of two diastereomers $\mathbf{4a}_{rac}$ and $\mathbf{4b}_{rac}$. Complete oxidation of the sulfide functional group in **4** was accomplished with *m*-CPBA to give sulfones $\mathbf{5a}_{rac}/\mathbf{5b}_{rac}$ (Scheme 1). Diastereomeric $\mathbf{5a}_{rac}/\mathbf{5b}_{rac}$ were subsequently separated by silica column chromatography, and their ratio was roughly 32:68. To continue the synthesis, we used the more abundant $\mathbf{5b}_{rac}$ diastereomer as compound $\mathbf{5a}_{rac}$ would not give the desired products. In an attempt to resolve racemic $\mathbf{5b}_{rac}$, we employed (1*S*,4*R*)-camphanic chloride.[54] Upon esterification of $\mathbf{5a}_{rac}$, two diastereomeric esters **6a**/**b** were separated by column chromatography (hexanes/EtOAc = 2:1) and then each independently reacted with sodium methoxide in order to remove the chiral auxiliary (Scheme 1); note that compounds **7** and now enantiopure **5b** were, from **6a**, obtained in a 1:9 ratio. Upon mesylation of enantiopure **5b** and then elimination of the mesyl group with non-nucleophilic DBU, we were able to isolate **8**; the enantiopurity of this compound was checked with chiral HPLC and found to have an ee > 99% (Figure S10, Supporting Information).[52] The treatment of compound **8** with *tert*-butyl isocyanoacetate, in the presence of *t*-BuOK (the Barton–Zard reaction), led to the formation of pyrrole derivative **9**. Hydrolysis of the *tert*-butyl ester functional group in **9** was optimized (70%) to give the corresponding carboxylic acid product; note that "deprotection" with trifluoroacetic acid (TFA) would give lower amounts (~40%) of the desired acid with competing decarboxylation product. The esterification of the product with coupling reagent PyBOP (benzotriazol-1-yloxytripyrrolidinophosphonium hexafluorophosphate) followed by $NaBH_4$ reduction gave pyrromethanecarbinol **10** (Scheme 1).

We used 0.395 mM *p*-TsOH in $CHCl_3$ for promoting the oligomerization of pyrromethanecarbinol **10** (5.0 mM, Scheme 2). The reaction allowed almost the exclusive formation of desired porphyrinogen that, upon oxidation with DDQ, gave octaester **11**. The cup-shaped octaester was isolated by column chromatography (dichloromethane/methanol = 50:1) and then converted into gated basket **1** (Scheme 2).

**Spectroscopic and Conformational Characteristics of Gated Baskets.** We incorporated metal cations, Zn(II) and Mn(III), into gated basket **1** to form Zn(II)–**1** and Mn(III)–**1** (Figure 2A) and then completed the characterization of these compounds. The $^1H$ NMR spectrum of gated basket **1** (400 MHz, $CDCl_3$) showed of a set of resonances corresponding to a $C_{4v}$ symmetric species (Figure 2B). On the basis of our prior study,[39] we reasoned that the shuttling of the N–H protons

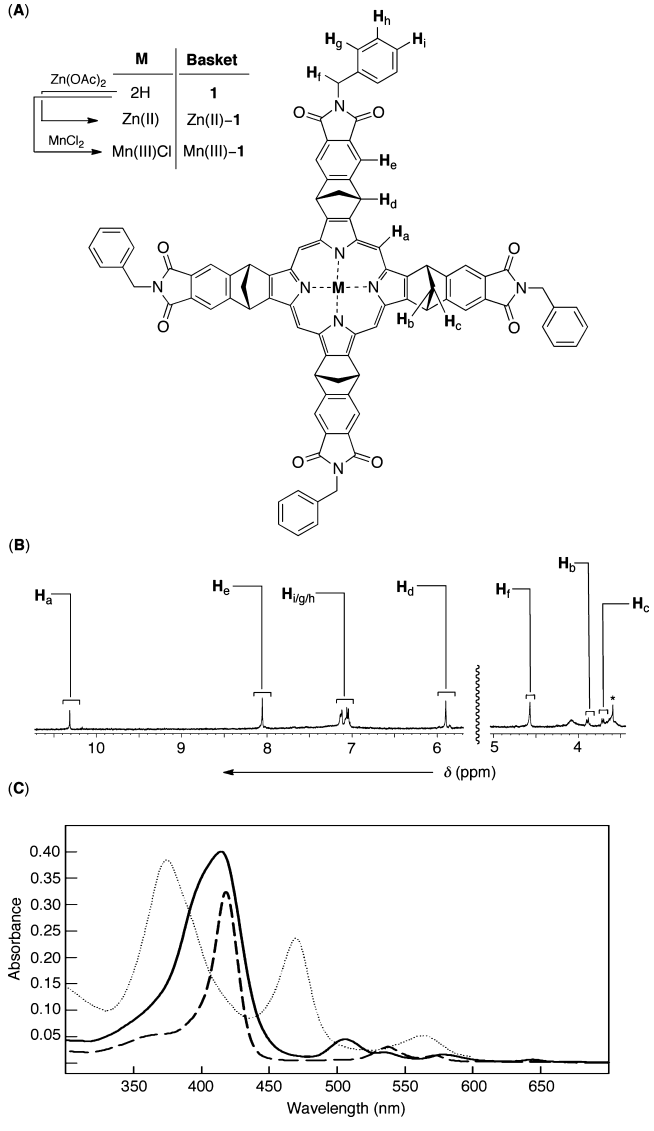


**Figure 2.** (A) Chemical structure of gated basket **1**, Zn(II)–**1**, and Mn(III)–**1**. (B) $^1H$ NMR spectrum (400 MHz, $CD_2Cl_2$) of basket Zn(II)–**1** at 298.0 K. (C) UV–vis spectra of gated basket **1** (0.005 mM, solid line), Zn(II)–**1** (0.003 mM, dashed line), and Mn(III)–**1** (0.004 mM, dotted line) in $CH_2Cl_2$ at 298 K.


dx.doi.org/10.1021/jo202443j | J. Org. Chem. 2012, 77, 2675–2688

was, at room temperature, fast enough for averaging the proton resonances. Indeed, variable-temperature (VT) $^1$H NMR study of **1** revealed decoalescence of all signals at ~228 K (Figure S40, Supporting Information),[52] corresponding to the expected change in the symmetry from $C_{4v}$ to $C_{2v}$ and the decelerated N−H shuttling. Moreover, the revolving of four benzene gates at the basket's entrance/exit must be accompanied with a small activation barrier, since the VT $^1$H NMR measurement did not show any additional change up to 194.2 K (Figure S40, Supporting Information).[52]

The porphyrin macrocycle has characteristics of an aromatic compound yet is flexible enough to adopt various nonplanar conformations.[55] The position of the Soret and Q bands in the electronic (UV−vis) spectrum of porphyrins is, in fact, indicative of the planarity of the ring: one typically identifies red shifts of the absorption bands originating from nonplanar deformations in the macrocycle.[56] The UV− vis spectra of free base **1**, Zn(II)−**1**, and Mn(III)−**1** baskets are shown in Figure 2C. Importantly, the $\lambda_{max}$ bands of **1** and Zn(II)−**1** are positioned at 645 and 572 nm (Figure 2C) and close to those measured for recently prepared free-base and Zn(II)−metalated bicyclic porphyrins ($\lambda_{max}$ = 665 and 551 nm);[57] these porphyrins were "equipped" with bicyclo[2.2.2]octene framework for increasing the system's rigidity and stabilizing the planar conformation in solution.[57] Moreover, the absorption bands in **1** and Zn(II)−**1** are blue-shifted with respect to the $\lambda_{max}$ of nonplanar octaethylporphyrins (for free-base and Zn(II)−OEP, $\lambda_{max}$ = 686 and 637 nm).[57,58] Another diagnostic feature of the distortion of the porphyrin macrocycle is the $^1$H NMR chemical shift of the N−H resonance appearing at a lower field than typically observed ($\delta$ = −2 to −5 ppm).[59] The chemical shift for the N−H protons in basket **1** were found at −4.97 ppm,[52] which in line with UV−vis measurements suggest that the base of our basket is indeed adopting a planar conformation in solution. The absorption spectrum of Mn(III)−**1** reveals two Soret bands at 374 and 470 nm (Figure 2C) and Q-band at 565 nm (Figure 2C). Importantly, the measured transitions are in the range of those reported for numerous Mn(III) porphyrins[48] further validating the incorporation of Mn(III) into basket **1**.

**$^1$H NMR Study of the Coordination of Imidazole-Based Ligands 12−14 to Zn(II)−1.** For promoting chemical reactions (epoxidation)[60] in the interior of gated baskets we decided to first investigate the axial coordination of imidazole-based ligands to Zn(II)−**1** and Mn(III)−**1** (Figure 3). The rationale for such studies rested in the notion that the coordination of *N*-heterocycles to the outer side of Mn(III)−**1** would enforce the chemical transformation to occur in the cavity of the basket.[61,62]

The cavity of gated basket **1** is sizable, and we used molecular mechanics (MM2) to estimate the volume of its inner space to be ~570 Å$^3$ (Figure 1B).[38] On the basis of their different size and shape, three imidazoles **12**−**14** (94−361 Å$^3$, Figure 3B) were anticipated to coordinate to inner and/or outer sides of Zn(II)−**1** (Figure 3A). We used $^1$H NMR spectroscopy to study the regioselectivity of the axial coordination: zinc(II) is in porphyrin systems diamagnetic ($d^{10}$ electronic state) and prone to form $ML_5$ square-pyramidal complexes suitable for $^1$H NMR studies.[63,64] The working hypothesis was based on our earlier work:[39] if the coordination of **12**−**14** to Zn(II)−**1** occurs on a particular side of the basket, *the magnetic environment of the nearby proton is perturbed to a greater extent* (Figure 3). For instance, a greater change in the chemical shift of the signal

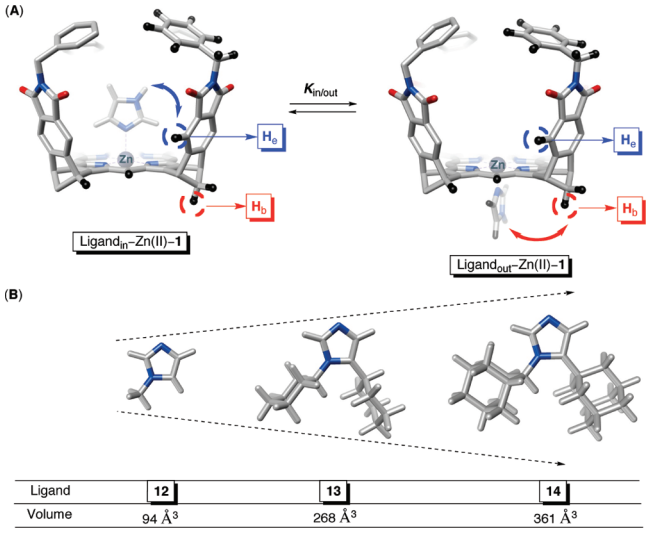


**Figure 3.** (A) Axial coordination of ligands **12**−**14**[52] could occur inside or outside of Zn(II)−**1**, and VT $^1$H NMR spectroscopy was used to quantify the equilibrium ($K_{in/out}$). (B) Chemical structures of energy minimized **12**−**14** (AM1, Spartan) and their corresponding volumes.

corresponding to outer $H_b$ protons (Figure 3A) should be diagnostic for the coordination occurring on the basket's outer side; in principle, measuring host−guest NOEs could give information about the position of the guest though we were unable to assign the guest's $^1$H NMR signals due to an extensive broadening and/or rapid exchange of its resonances. Accordingly, we titrated **12**−**14** (~13 mM) to Zn(II)−**1** (0.15 mM) in $CD_2Cl_2$ and recorded $^1$H NMR spectrum (400 MHz, 298.0 K) upon each addition of the ligand (Figures S11−S19, Supporting Information).[52] Then, we plotted the relative change in the chemical shift ($\Delta\delta$, ppm) of protons $H_b$ (located on the basket's outer side, Figure 3A) and $H_e$ (located on the basket's inner side, Figure 3A) as a function of the molar equivalents of **12**−**14** (Figure 4). Evidently, the binding of smaller 1-methylimidazole **12** to Zn(II)−**1** caused a greater perturbation of the magnetic environment of the inner $H_e$ protons ($\Delta\delta$ = 0.04 ppm, Figure 4A).

The coordination of more sizable **14** to Zn(II)−**1**, however, caused a more considerable perturbation of the outer $H_b$ protons ($\Delta\delta$ = 0.06 ppm, Figure 4C). Despite rather small perturbations ($\Delta\delta$ < 0.1), there still exists a trend in the relative change of the chemical shifts ($\Delta\delta$, Figure 4) of $H_e$ and $H_b$: the more sizable the ligand the greater the $^1$H NMR chemical shift of the outer protons and vice versa! A useful way to visualize the trend is to view the blue and red curves in Figure 4 from left to right. It subsequently follows that at 298.0 K smaller **12** (94 Å$^3$) prefers coordinating to the inner while bigger **14** (361 Å$^3$) to the outer side side of Zn(II)−**1** (Figure 5).

For quantifying the observed in/out stereoisomerism, we used variable-temperature $^1$H NMR spectroscopy (Table 1). The chemical exchange of ligands **12**−**14** to and from Zn(II)−**1** was, at low temperatures, expected to slow down with a decoalescence of proton resonances corresponding to the formation of in/out stereoisomers (Figure 3A). Indeed, variable-temperature $^1$H NMR measurements (400 MHz, $CD_2Cl_2$) of **13**−Zn(II)−**1** and **14**−Zn(II)−**1** (~190−220 K) showed two sets of resonances with the integration ratio being a function of the external temperature (Figures S22−S25, Supporting Information).[52] The integration of the signal


dx.doi.org/10.1021/jo202443j | J. Org. Chem. 2012, 77, 2675−2688

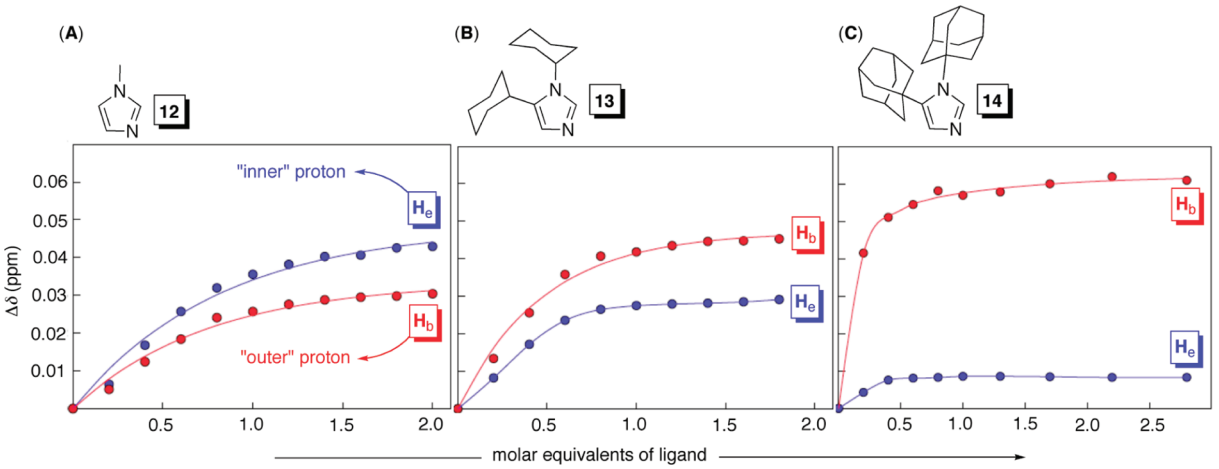


**Figure 4.** Relative $^1$H NMR (400 MHz, 298.0 K) chemical shifts ($\Delta\delta$, ppm) of $H_e/H_b$ protons in Zn(II)−**1** measured upon incremental addition of variously sized ligands **12**−**14** to its $CD_2Cl_2$ solution.[52].

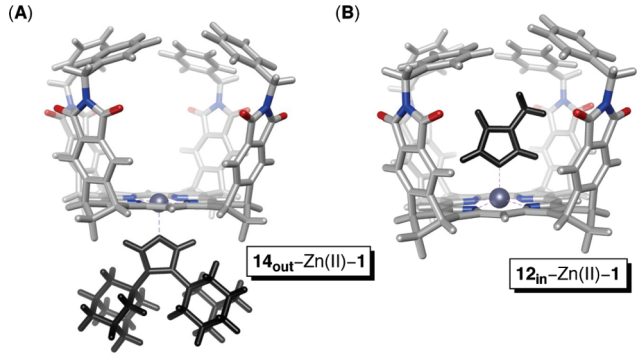


**Figure 5.** Chemical structures of energy-minimized (AM1, Spartan) $14_{out}$−Zn(II)−**1** (A) and $12_{in}$−Zn(II)−**1**.

**Table 1. Thermodynamic Parameters for Stereoisomeric In/Out Equilibration ($K_{in/out}$ = [out]/[in]) of Complexes (13/14)−Zn(II)−1 Generated from VT $^1$H NMR Measurements and van't Hoff Analysis[a]**

| ligand | $K_{in/out}$[d] | $\Delta H^\circ_{in/out}$ (kcal/mol) | $T\Delta S^\circ_{in/out}$[d] (kcal/mol) | % In[d] | % Out[d] |
|---|---|---|---|---|---|
| **12**[b] | | | | ~100 | 0 |
| **13** | 0.99 | 0.55 ± 0.03 | 0.54 ± 0.03 | 50 | 50 |
| **14**[c] | 6.5 | 1.44 ± 0.09 | 2.55 ± 0.20 | ~10 | ~90 |

[a]Figure S26 (Supporting Information), $R^2$ = 0.98 for **13** and $R^2$ = 0.97 for **14**).[51]. [b]VT $^1$H NMR showed no decoalescence of resonances. [c]The estimated percentage of *in* and *out* stereoisomers changes to 0:100 if one plots % (out) as a function of temperature (linear dependence, $R^2$ = 0.99). [d]At 298.0 K.

corresponding to $H_e$ protons (with the ligand coordinated on the inner $\delta_{in}$ = 7.97 ppm and the outer side $\delta_{out}$ = 8.03 ppm)[52] in both **13**−Zn(II)−**1** and **14**−Zn(II)−**1** allowed us to evaluate the proportion of in/out stereoisomers and create the corresponding van't Hoff plots (Figure S26, Supporting Information, Table 1).[52]

Markedly, 1,5-dicyclohexylimidazole **13** would at 298.0 K coordinate to both inner and outer sides of Zn(II)−**1**, while the larger 1,5-diadamantylimidazole **14** would preferentially reside at the outer side of Zn(II)−**1** (Table 1). A set of $^1$H NMR resonances (298.0 K) corresponding to the coordination complex **12**−Zn(II)−**1** was unaltered at all temperatures (for $H_e$, $\delta_{in}$ = 7.95 ppm; see Figure S21, Supporting Information), indicating the exclusive formation of $\mathbf{12}_{in}$−Zn(II)−**1** (Table 1).

Apparently, there is an enthalpic $\Delta H^\circ_{in/out}$ but not entropic $\Delta S^\circ_{in/out}$ advantage (see Table 1) for ligands **13** and **14** coordinating to the inner side of Zn(II)−**1**. The situation is different from previously examined cup-shaped baskets[39] whereby the entropically favorable desolvation of ligands would allegedly drive their coordination to the inner side. We surmise that in the case of Zn(II)−**1**, the extended phthalimide "side walls" as well as the revolving gates (absent in cup-shaped baskets) interact with the entrapped guest, thereby affecting the enthalpy/entropy balance in the binding.

Preliminary computational study of the in/out stereoisomerism (DFT, RI-BP86/SV(P), TZVP)[52,65−68] furthermore revealed a somewhat greater affinity of **12** ($\Delta E_{out/in}$ = −3.60 kcal/mol) over **13** ($\Delta E_{out/in}$ = −2.61 kcal/mol) or **14** ($\Delta E_{out/in}$ = −1.91 kcal/mol) for residing in the interior of Mn(III)−**1**. The origin of the trend for the computed energy difference ($\Delta E$) rests in the van der Waals strain increasing in the series $\mathbf{12}_{in}$−**Mn**(III)−**1** < $\mathbf{13}_{in}$−**Mn**(III)−**1** < $\mathbf{14}_{in}$−**Mn**(III)−**1**: the distance between the two opposite phthalimide "side walls" is in $ligand_{in}$−Mn(III)−**1** increasing with more sizable ligands[51] therefore indicating adverse steric interactions. In fact, one needs to take the solvation as well as dynamics of the host/guest pair into an account to obtain more information on the binding thermodynamics.

**Quantitative Study of the Coordination of 12/14 to Metalloporhyrins.** With a good understanding of the in/out stereoisomerism, we used UV−vis spectroscopy for quantifying the binding affinity of **12** and **14** toward Zn(II)−**1** and Mn(III)−**1** as well as metalloporphyrins **15**−**17** (Figure 6). Since 1,5-dicyclohexylimidazole **13** would, at room temperature, coordinate to both inner and outer sides of Zn(II)−**1**, we refrained from quantifying the axial binding of this particular compound. The modes of the complexation of Zn(II) and Mn(III) porphyrins with *N*-heterocycles, forming five- and six-coordinate species (Figure 6A), are described in the literature[63,69−73] and as such used in our analysis. The coordination of **12** and **14** to Zn(II)−**1** ($CH_2Cl_2$, 298.0 K) affected both the Soret and Q absorption bands of the porphyrin chromophore (Figure 6B); note that the red (10−15 nm) shift of the Soret band is typically observed for *N*-heterocycles binding to Zn(II) porphyrins.[74,75] The appearance


dx.doi.org/10.1021/jo202443j | J. Org. Chem. 2012, 77, 2675−2688

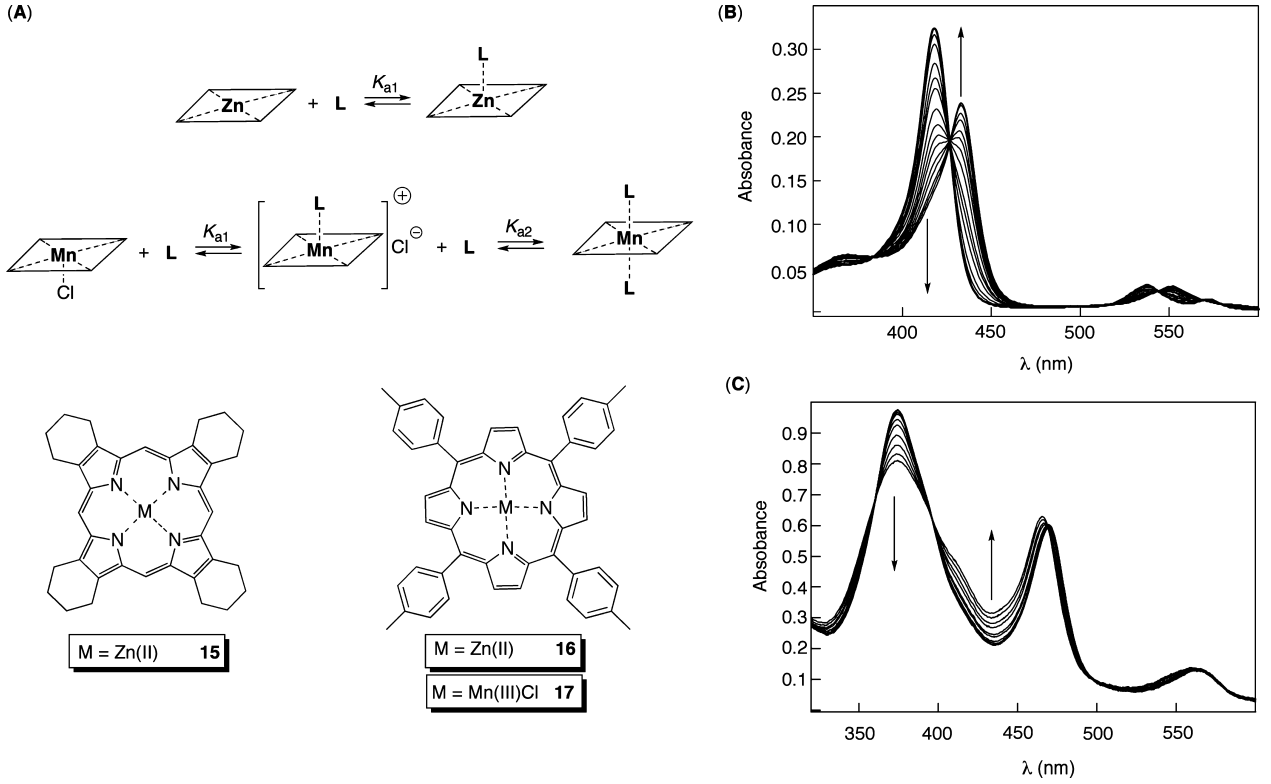


**Figure 6.** (A) Two modes of binding of imidazole-based ligands (L) to Zn(II) and Mn(III) porphyrins[63,69−73] (top) and chemical structure of **15**−**17** (bottom).[52] (B) UV−vis spectra of Zn(II)−**1** (0.0026 mM, $CH_2Cl_2$) recorded upon an incremental addition of a solution of **14** (up to 1000 molar equiv) at 298.0 K. (C) UV−vis spectra of Mn(III)−**1** (0.029 mM, $CH_2Cl_2$) recorded upon an incremental addition of a solution of **14** (up to 1000 molar equiv) at 298.0 K.

**Table 2. Thermodynamic Stability Constants ($K_{a1}$ and $K_{a2}$ at 298.0 K) Characterizing 12 and 14 Complexation to Zn(II) and Mn(III) Porphyrins Obtained by Multivariate Factor Analysis of the UV−vis Titration Data[52]**

| | 1-methylimidazole (**12**) | | 1,5-diadamantylimidazole (**14**) | |
|---|---|---|---|---|
| porphyrin | $K_{a1}$ ($M^{-1}$) | $K_{a2}$ ($M^{-1}$) | $K_{a1}$ ($M^{-1}$) | $K_{a2}$ ($M^{-1}$) |
| **15**[a] | $4.0 \pm 0.2 \times 10^3$ | | $5.1 \pm 0.3 \times 10^3$ | |
| **16**[a] | $1.78 \pm 0.04 \times 10^4$ | | $3.7 \pm 0.1 \times 10^4$ | |
| Zn(II)−**1** | $4.46 \pm 0.09 \times 10^4$ | | $1.91 \pm 0.07 \times 10^5$ | |
| **17** | 58 ± 12 | 45 ± 22 | 68 ± 18 | <10 |
| Mn(III)−**1** | 58 ± 13 | <5 | 332 ± 26 | 0[b] |

[a]For a direct comparison of these data, we applied statistical correction $K_{a1} = 1/2\ K_{(experimental)}$.[78,79] [b]The coordination of the second ligand was not observed.

of isosbestic points is, in our experiments (Figure 6B), indicative of **14** (but also **12**, Figure S33, Supporting Information)[52] exclusively coordinating to one side of Zn(II)−**1** (at 298.0 K). The UV−vis titration data were subjected to multivariate factor analysis (Figures S27−S36, Supporting Information, ReactLab EQUILIBRIA software)[52] for obtaining equilibrium constant $K_{a1}$ (Table 2).[76,77] Interestingly, the affinity of **12**/**14** toward Zn(II)−**1** is somewhat greater than toward "flat" porphyrins **15** and **16** (Table 2). Furthermore, 1,5-diadamantylimidazole **14** has a greater propensity for coordinating zinc(II) porphyrins than 1-methylimidazole **12** (Table 2). *N*-Heterocycles are known to bind to Mn(III) porphyrins forming five- and six-coordinate complexes (Figure 6A);[69−73,80−85] in case of Mn(III)−**1**, the heterocycle should displace the coordinated chloride anion (Figure 2A). The literature precedents would, in addition, suggest that the thermodynamic stability of Mn(III) complexes is (a) a function of the porphyrin's counterion (Figure 2A) and (b) typically smaller than that of the corresponding zinc(II) porphyrins. An incremental addition of 1,5−diadamantylimidazole **14** to Mn(III)−**1** led to distinct UV−vis spectroscopic changes, resembling the results of the titration of the Collman's picnic basket[84] (Figure 6C). Importantly, the appearance of several isosbestic points suggested that two colored species, e.g. the metalated basket and its 1:1 complexed form, contributed to the recorded spectra (Figure 6C); the result bodes well with the finding that large guest **14** prefers coordinating to one (the outer) side of Zn(II)−**1**. For other titrations involving Mn(III) porphyrins (Table 2), no isosbestic point(s) were observed,[69] suggesting the formation of both 1:1 ($K_{a1}$, Figure 6A) and 1:2 ($K_{a2}$, Figure 6A) complexes.[52] In these experiments,[52] rather small and insufficient UV−vis spectroscopic changes accompanied the complexation events (Figures S31/32 and S35/36, Supporting Information), thus complicating the binding analysis[82] and contributing to a greater uncertainty of the stability constants $K_{a1}$ and $K_{a2}$ (Table 2).


dx.doi.org/10.1021/jo202443j | J. Org. Chem. 2012, 77, 2675−2688

**Working Hypotheses about the Epoxidation of Alkenes with Gated Baskets.** The interior of concave hosts could accommodate complementary guests and, in some cases even alter the course of chemical reactions.[5,11,86,87] In particular, the confined environment of hosts can modulate the energy landscape of encapsulation reactions having an effect on the stability of reactive intermediates[9] and/or transition states[14] thereby affecting the rate, overall yield, product distribution and stereoselectivity.[11] One of the basic features of the encapsulation catalysis is so-called shape selectivity:[88] the catalyst promotes a faster conversion of substrates with size/shape complementary to its inner space.[89−91] For example, "picnic basket" (Figure 7A) was designed to comprise a

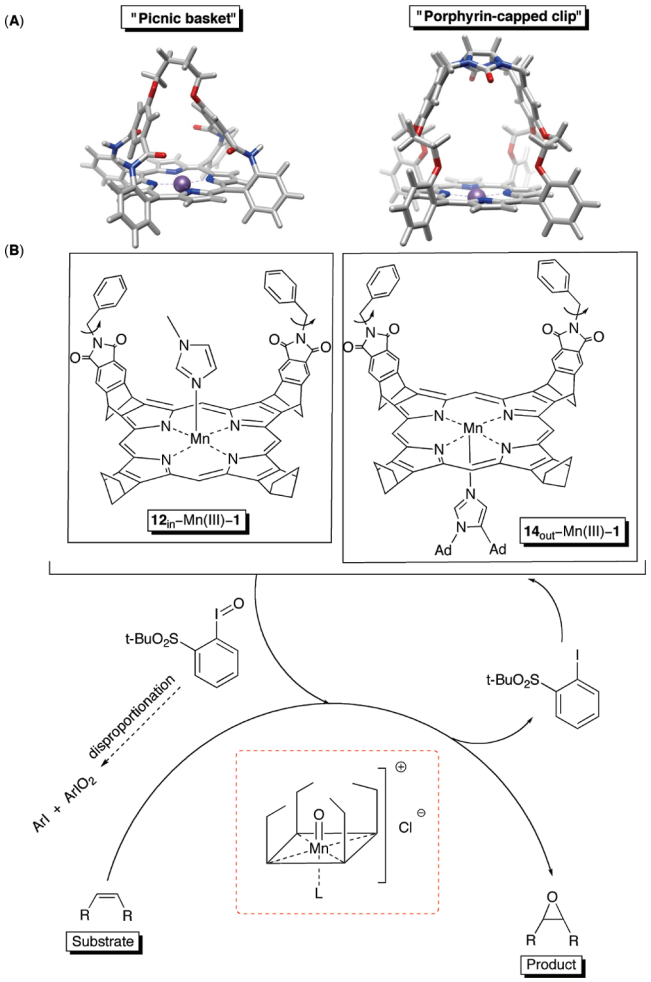


**Figure 7.** (A) Energy-minimized forms (MMFF, Spartan) of Collman's picnic basket[61] and Nolte's porphyrin-capped clip.[92] (B) Epoxidation of alkenes, with the assistance of terminal iodosylarene, had been envisioned to occur in the interior of $\mathbf{14}_{out}$–Mn(III)–**1** and at the outer face of $\mathbf{12}_{in}$–Mn(III)–**1**.

Mn(III)–porphyrin "floor" and two isophthaloyl-based "side walls" forming a cavity whose size could be adjusted via synthesis.[61,84,93] Remarkably,[44] this compound promoted shape-selective epoxidation of alkenes in its interior. The picnic basket and more recently developed porphyrin-capped clip[82,94] (Figure 7A), however, each have a molecular framework requiring considerable synthetic effort for installing gates and thereby controlling the constrictive binding energy[17] of guests.

The cavity of gated basket **1** is sizable (Figure 1B, ~570 Å$^3$)[37,95] so that numerous guests populating ~55% of its space may reside in the interior.[38] Along with this notion, we decided to investigate the catalytic epoxidation of alkenes with Mn(III)–**1** having a heterocyclic ligand complexed at its outer ($\mathbf{14}_{out}$–Mn(III)–**1**) or inner ($\mathbf{12}_{in}$–Mn(III)–**1**) side (Figure 7B). On the basis of earlier mechanistic studies,[47−49] we reasoned that our Mn(III) baskets (~570 A$^3$) should give rise to a reactive Mn(V)=O species in the presence of iodosylarene (*t*-BuSO$_2$PhIO/236 Å$^3$, Figure 7B). This low spin (Mn(V) is d$^2$ with $S$ = 0) intermediate should, in turn, be capable of transferring its oxygen atom to an alkene and form the corresponding epoxide.[95] In this way, basket $\mathbf{14}_{out}$–Mn(III)–**1** would form the elusive oxo intermediate on the interior of the cavity, while in $\mathbf{12}_{in}$–Mn(III)–**1**, the oxygen transfer moiety would be outside of the cavity; importantly, the counter chloride anion is in these complexes noncoordinating.[63,69−73] The oxygen transfer reaction should thus be possible to occur on either face of the metalated porphyrin (Figure 7B). Given a particular regio-, stereo-, and shape-selectivity of such epoxidations,[44,96−99] one should be able to draw a conclusion about the transformation occurring in the interior of $\mathbf{14}_{out}$–Mn(III)–**1** (Figure 7B). Note that the four aromatic gates are expected to restrict the rate by which alkenes reach the embedded catalytic center.

To test our working hypotheses, we studied the regio and stereoselectivity of the epoxidation of four differently sized olefins **18**–**21** (Figure 8A) using baskets $\mathbf{12}_{in}$–Mn(III)–**1** and $\mathbf{14}_{out}$–Mn(III)–**1** (Figure 7B), and model catalyst **17** (Figure 6).

**Epoxidation of (*R*)-Limonene 18.** (*R*)-Limonene **18** contains one stereocenter and two double bonds (Figure 8A). While most oxidizing reagents predominantly epoxidize more substituted (internal) alkene functionality (pathway a, Figure 8B),[100] sterically hindered Mn(III)–porphyrins were shown to prefer functionalizing the external double bond (pathway b, Figure 8B).[101] The sizable cavity of $\mathbf{14}_{in}$–Mn(III)–**1** (~570 Å$^3$) should easily accommodate **18** (176 Å$^3$), though we were still curious about the regio-/diastereoselectivity of the epoxidation.

All reactions were completed in $CH_2Cl_2$ at 298 K, at which point ligands **12** and **14** were found to coordinate to the inner and outer sides, respectively, of Mn(III)–**1** (Table 2). Small solvent molecules ($CH_2Cl_2$, 61 Å$^3$) were assumed to have negligible affinity for the interior of the basket and therefore be poorly competitive with (*R*)-limonene **18** as guests. The excessive amounts of alkene (6000 molar equiv) were used to suppress the rapid disproportionation of iodosylarene (Figure 7B).[45] The amount of imidazole-based ligands **12**/**14** (500–1000 molar equiv) was chosen to saturate Mn(III)–**1** (0.05 mM, Table 2) under experimental conditions. The formation of $\mu$-oxo dimers of Mn(III)–porphyrins has been known to contribute to their decomposition[102] although the unique topology of our Mn(III)–**1** basket improved the catalyst's stability as was also exemplified by Nolte's clip-shaped porphyrins (Figure 7A).[94] The epoxidation of (*R*)-limonene **18** (0.3 M) with Mn(III)–**1** (0.05 mM) was thus repeated, with three consequent additions of iodosylarene (5.0 mM) to reveal a small drop (5–10%) in the overall yield of the epoxide.

The epoxidations of (*R*)-limonene **18** with $\mathbf{12}_{in}$–Mn(III)–**1** and $\mathbf{14}_{out}$–Mn(III)–**1** were found to have identical outcomes (Table 3). Accordingly, if the chemical transformation occurred inside $\mathbf{14}_{out}$–Mn(III)–**1** then the reaction's energetics would


dx.doi.org/10.1021/jo202443j | J. Org. Chem. 2012, 77, 2675–2688

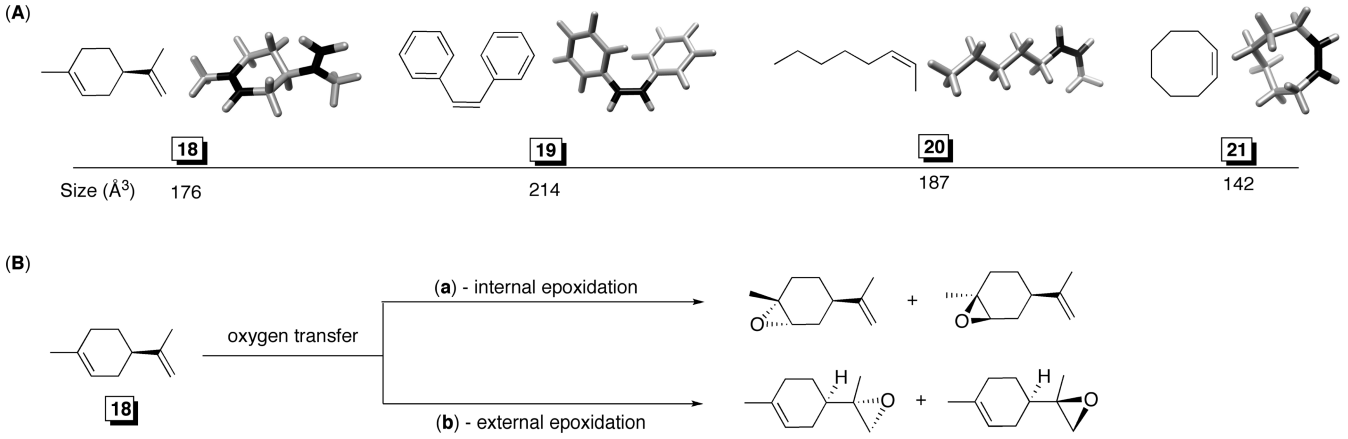


**Figure 8.** (A) Chemical structures of alkenes **18**–**21** having different size and shape (AM1). (B) Epoxidation of (*R*)-limonene **18** occurs at the (a) internal or (b) external double bond.

**Table 3. Epoxidation of (*R*)-Limonene 18 (0.3 M) Completed in $CH_2Cl_2$ (298 K) with Iodosylarene (5.0 mM) and Porphyrin (0.05 mM) (Alkene/ArIO/Porphyrin = 6000:100:1)[a]**

| porphyrin system | epoxidation regioselectivity[d] | internal diastereoselectivity[e] | external diastereoselectivity[e] |
|---|---|---|---|
| **12**–**17**[b] | 4.81 ± 0.01 | 1.12 ± 0.01 | 1.27 ± 0.01 |
| **12**–**17**[c] | 4.81 ± 0.03 | 1.12 ± 0.01 | 1.29 ± 0.02 |
| $\mathbf{12}_{in}$–Mn(III)–**1**[b] | 3.94 ± 0.01 | 1.04 ± 0.01 | 1.47 ± 0.01 |
| $\mathbf{14}_{out}$–Mn(III)–**1**[b] | 4.04 ± 0.01 | 1.11 ± 0.01 | 1.40 ± 0.01 |

[a]The progress of the epoxidation was monitored with quantitative gas chromatography (GC) with error bars presenting standard deviation from two measurements. [b]500 molar equiv of the ligand. [c]1000 molar equiv of the ligand. [d]GC was used to determine the ratio of [internal epoxide]/[external epoxide]. [e]GC was used to determine the ratio of diastereomeric epoxides.

simply be indistinguishable from the one taking place at the outer face of $\mathbf{12}_{in}$–Mn(III)–**1**. At this point, we only deduced that the spacious cavity of the basket had no effect on the chemical behavior of this particular reactant and decided to consider the epoxidation of *more* sizable *cis*-stilbene **19** (214 Å$^3$, Figure 8A). A somewhat different outcome of the epoxidation of **18** with "flat" porphyrin **17** (Table 3) can be accounted for by considering distinct electronic and steric characteristics of the two catalysts.[81]

**Epoxidation of *cis*-Stilbene 19.** The catalytic epoxidation of *cis*-stilbene **19** with manganese(III) porphyrins gives rise to *cis*- but also *trans*-2,3-diphenyloxirane (Figure 9).[81,82,94] Typically, the reaction is, in the presence of various terminal oxidants, diastereoselective with predominant formation of the *cis* product and the retention of stereochemistry.[103−105] In fact, the stepwise transfer of oxygen atom[81,106] occurs at a faster rate and with a greater stereoselectivity in the presence of strong $\sigma$-donating ligands (L, Figure 9).[82] It has, accordingly, been proposed that the axial coordination has an effect on the position of the manganese atom with respect to the porphyrin ring: the stronger the coordination the closer the manganese atom to the porphyrin ring and the greater the stereoselectivity.[82,107] The epoxidations of *cis*-stilbene **19** (0.3 M) with $\mathbf{12}_{in}$–Mn(III)–**1** and $\mathbf{14}_{out}$–Mn(III)–**1** (0.05 mM) were completed in the presence of iodosylarene (5.0 mM) in $CH_2Cl_2$ at room temperature. The yields of the two reactions, with respect to the terminal oxidant, were comparable (~50%) although the stereoselectivity was somewhat different (Table 4). The epoxidation occurring in the cavity of $\mathbf{14}_{out}$–Mn(III)–**1** would, to a greater degree, favor the formation of the *trans* product (*cis*/*trans* = 6.6:1, Table 4). On the other hand, the reaction occurring at the outer face of $\mathbf{12}_{in}$–Mn(III)–**1** gave less of the *trans* epoxide (*cis*/*trans* = 8.6: 1, Table 4). Importantly, model porphyrin systems **12**/**14**–**17** promoted the epoxidation of **19** with the stereoselectivity of *cis*/*trans* ~12.5:1 (Table 4) whereby ligands **12** and **14** had no measurable effect on the stereoisomeric product ratio!

On the basis of the results of the epoxidation of compounds **18** (176 Å$^3$) and **19** (214 Å$^3$), it follows that the conversion of more sizable *cis*-stilbene **19** is indeed taking place in the interior of $\mathbf{14}_{out}$–Mn(III)–**1**. The cavity of the basket has a small, yet measurable, effect on the thermodynamic stability of the

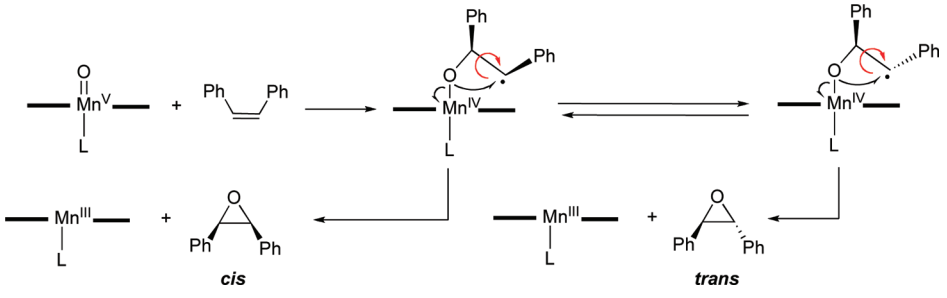


**Figure 9.** Epoxidation of *cis*-stilbene with Mn(III) porphyrins is apparently a stepwise process.[81,82,105]


dx.doi.org/10.1021/jo202443j | *J. Org. Chem.* 2012, 77, 2675−2688

**Table 4. Epoxidation of *cis*-Stilbene 19 (0.3 M) Completed in $CH_2Cl_2$ (298 K) with Iodosylarene (5.0 mM) and Porphyrin (0.05 mM) (Alkene/ArIO/Porphyrin = 6000:100:1)[a]**

| porphyrin system | *cis*/*trans* epoxide[d] | overall yield[d] (%) |
|---|---|---|
| **12**–**17**[b] | 11 ± 1 | 73 |
| **12**–**17**[c] | 12.5 ± 0.2 | 71 |
| **14**–**17**[b] | 12.3 ± 0.1 | 76 |
| $\mathbf{12}_{in}$–Mn(III)–**1**[b] | 8.7 ± 0.1 | 49 |
| $\mathbf{12}_{in}$–Mn(III)–**1**[c] | 8.6 ± 0.1 | 47 |
| $\mathbf{14}_{out}$–Mn(III)–**1**[b] | 6.6 ± 0.3 | 49 |

[a]The progress of the epoxidation was monitored with quantitative gas chromatography (GC) with error bars presenting the standard deviation from two measurements. [b]500 molar equiv of the ligand. [c]1000 molar equiv of the ligand. [d]Two GC measurements were completed to determine the reaction's stereoselectivity and overall yield.

reaction's transition states and intermediates (Figure 9), thereby leading to the formation of two diastereomeric products in the observed ratio (Table 4); somewhat smaller quantity of *cis*-stilbene produced inside the host is indeed intriguing, and perhaps due to the inner space stabilizing the transition state leading to the *trans* compound.

**Competitive Epoxidation of *cis*-2-Octene 20 and *cis*-Cyclooctene 21.** What would be the outcome of two concurrent epoxidations of alkenes having different shape/size inside the basket's cavity? Olefins **20** (*cis*-2-octene, 187 Å$^3$, Figure 8A) and **21** (*cis*-cyclooctene, 142 Å$^3$, Figure 8A) could both easily occupy the interior of gated **1** (570 Å$^3$, Figure 10). To evaluate the ability of the basket for kinetically resolving **20** from **21**, we completed the epoxidation of their equimolar mixture (0.15 M each) with $\mathbf{12}_{in}$–Mn(III)–**1** and $\mathbf{14}_{out}$–Mn(III)–**1** (0.05 mM) in $CH_2Cl_2$ at room temperature; note that the term "kinetic resolution" is more precisely used for describing two enantiomers reacting at different rates and giving rise to predominantly one product.[108]

Notably, the epoxidation of equimolar **20**/**21** at the outer face of $\mathbf{12}_{in}$–Mn(III)–**1** led to the formation of linear/cyclic epoxides in the ratio 1.2:1 (Table 5). When the same reaction

**Table 5. Epoxidation of Equimolar 20/21 (0.15 M Each) Completed in $CH_2Cl_2$ (298 K) with Iodosylarene (5.0 mM) and Porphyrin System (0.05 mM)[a]**

| porphyrin system | *cis*/*trans* epoxide[c] | **20**/**21** product ratio[c] | overall yield[c] (%) |
|---|---|---|---|
| **12**–**17**[b] | 9.56 ± 0.01 | 1.27 ± 0.01 | >90 |
| **14**–**17**[b] | 9.31 ± 0.07 | 1.27 ± 0.01 | >90 |
| $\mathbf{12}_{in}$–Mn(III)–**1**[b] | 6.6 ± 0.3 | 1.2 ± 0.1 | 82 |
| $\mathbf{14}_{out}$–Mn(III)–**1**[b] | 6.4 ± 0.2 | 2.0 ± 0.1 | 68 |

[a]The progress of the epoxidation reactions was monitored with quantitative gas chromatography (GC) with error bars presenting the standard deviation from two measurements. [b]500 molar equiv of the ligand. [c]GC was used to determine the ratio of [*cis*]/[*trans*]-2-methyl-3-pentyloxirane obtained from *cis*-2-octene **20**. We used quantitative GC for obtaining the product ratio and overall reaction yield.

was promoted with model systems **12**–**17** and **14**–**17**, we measured the comparable selectivity of 1.27:1 (Table 5).[61]

The epoxidation within the interior of $\mathbf{14}_{out}$–Mn(III)–**1**, however, gave greater quantities of the linear epoxide: the ratio of the linear to cyclic epoxide products was found to be 2.0:1 (Table 5).

The fact that the epoxidation of equimolar **20**/**21** had, in the presence of catalysts $\mathbf{12}_{in}$–Mn(III)–**1** and $\mathbf{14}_{out}$–Mn(III)–**1**, a different outcome is in line with the notion that the reaction is indeed taking place in two distinct environments. That is to say, the epoxidation with $\mathbf{12}_{in}$–Mn(III)–**1** occurs at its outer side while with $\mathbf{14}_{out}$–Mn(III)–**1** in the basket's cavity. In addition, the epoxidation of linear alkene **20** appears somewhat faster (or cyclic **21** slower) in the interior of $\mathbf{14}_{out}$–Mn(III)–**1** (Table 5); the observed effect is small but quantifiable from multiple measurements. What is the origin of the observed "shape selectivity"?[61,96,99]

First, we examined the host–guest interaction of (*R*)-limonene **18** and basket **1** using $^1$H NMR spectroscopy.[52] Upon an incremental addition of (*R*)-limonene (2.0–30.0 molar equiv) to the basket (0.67 mM) dissolved in $CH_2Cl_2$ (298.0 K), there was no observable change in the chemical shift of any proton resonance (Figure S37, Supporting Information).

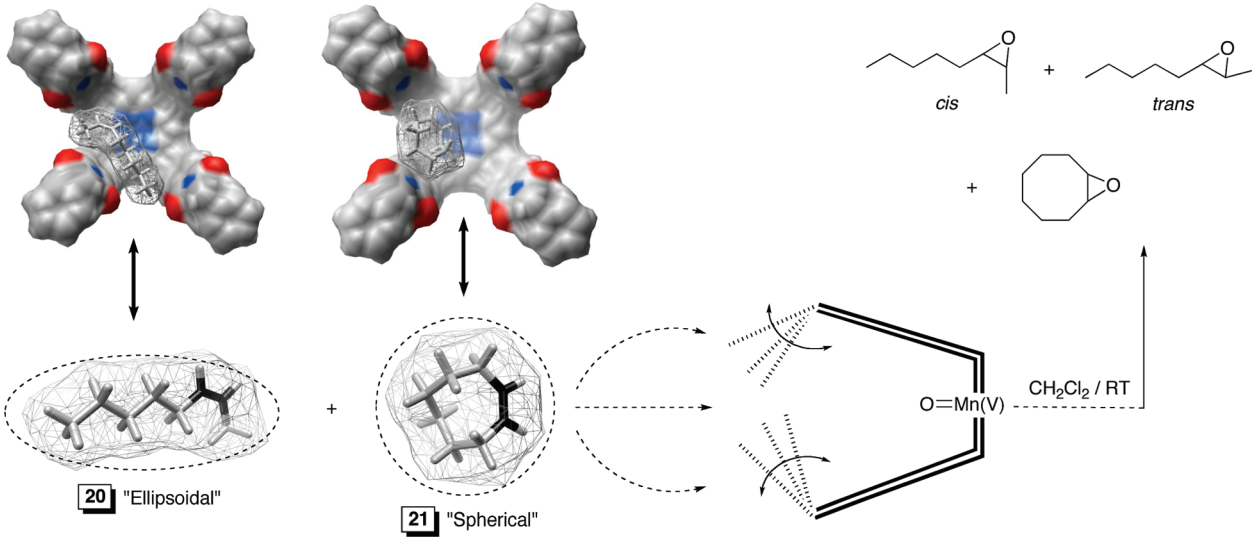


**Figure 10.** Molecular sufaces of energy-minimized (MMFF) structures of **20** and **21** docked in the interior of gated basket **1** (left). In reaching the interior of $\mathbf{14}_{out}$–Mn(III)–**1**, olefins **20** and **21** pass the revolving gates at the rim of the basket (right).


dx.doi.org/10.1021/jo202443j | J. Org. Chem. 2012, 77, 2675–2688

One can, accordingly, estimate[76] that guest **18** (176 Å$^3$) has a rather negligible affinity (if any, $K_a$ < 10 M$^{-1}$) for occupying the sizable cavity of host **1** (570 Å$^3$). As shown earlier (Table 3), the epoxidation of (*R*)-limonene occurred in the interior of **14**$_{out}$−Mn(III)−**1** with regio- as well as diastereoselectivity identical to the reaction at the outer side of **12**$_{in}$−Mn(III)−**1**. Altogether, the binding and the reactivity studies suggest that alkene **18** is likely adopting various isoenergetic orientations inside spacious **14**$_{out}$−Mn(III)−**1**. Subsequently, we completed $^1$H NMR titration of similarly sized *cis*-2-octene **20** (187 Å$^3$) and *cis*-cyclooctene **21** (142 A$^3$) to basket **1** (Figures S38/S39, Supporting Information), to reveal that these two alkenes have negligible affinity (if any, $K_a$ < 10 M$^{-1}$) for occupying the cavity of the basket (570 Å$^3$). Given that the gated basket has no measurable propensity for complexing alkenes **20**/**21**, could the observed kinetic resolution of such compounds emanate from the catalyst's topology and/or its dynamic nature (gating) in which linear guest **20** has a greater access to the embedded catalytic site in gated **14**$_{out}$−Mn(III)−**1** than the spherical **21** (Figure 10)?[109]

Small energetic changes that characterize the competition reaction make any quantitative evaluation of the mechanism a challenging task. For instance, if one guest (**20** or **21**) has an affinity of $K_a$ = 5 M$^{-1}$ and another $K_a$ = 2 M$^{-1}$ toward **14**$_{out}$−Mn(III)−**1**, then $\Delta\Delta G°$ would at 298 K be 0.54 kcal/mol; on the basis of the observed reaction's selectivity, however, one estimates that the rate difference for the oxidation of **20**/**21** amounts to $\Delta\Delta G^{‡}$ ∼0.3 kcal/mol (Table 5). Evidently, additional studies are needed to examine the validity of the discussed mechanistic scenarios as well as evaluate the potential of a dynamic control of the outcome of a chemical reaction occurring in a gated environment.

## CONCLUSIONS

Dynamic control of substrate access to a catalytic center, embedded in a synthetic molecular cavitand, could presumably have an effect on the outcome of chemical reaction taking place in such a confined space. We designed, prepared and investigated the catalytic behavior of a new family of gated baskets[15] comprising a porphyrin "floor" fused to four phthalimide "side walls" and each carrying a revolving aromatic "gate". *These rather spacious supramolecular catalysts (∼570 Å$^3$) were hereby shown to* promote the epoxidation of alkenes (142−214 Å$^3$) in their interior. Despite the fact that the measured catalytic characteristics of the basket are still far from being useful for any particular synthetic application, the unique topology and dynamic nature of gated catalysts are certainly worth exploring for directing the outcome of chemical reactions. It is shown, therefore, that the results described in this study are important for learning about the relationship between the process of gating[15] and chemical reactions occurring in confined environments.

## EXPERIMENTAL SECTION

**General Methods.** All chemicals were purchased from commercial sources and used as received unless stated otherwise. All solvents were dried prior to use according to standard literature procedures. Chromatography purifications were performed using silica gel 60 ($SiO_2$, 40−75 μm, 200 × 400 mesh). Thin-layer chromatography (TLC) was performed on silica gel plate w/UV254 (200 μm). Chromatograms were visualized by UV light and stained using 20% phosphomolybdic acid in ethanol, if needed. $^1$H and $^{13}$C NMR spectra were recorded, at 400 and 100 MHz respectively. They were referenced using the solvent residual signal as an internal standard. The chemical shift values are expressed as δ values (ppm) and the couple constants values (*J*) are in Hertz (Hz). The following abbreviations were used for signal multiplicities: s, singlet; d, doublet; t, triplet; m, multiplet; and br, broad.

**Compound 3.** A solution of *m*-CPBA (4.4 g, 70%, 18.0 mmol) in dichloromethane (50.0 mL) was added to a solution of compound **2** (3.1 g, 12 mmol) in dichoromethane (50.0 mL) at 0 °C. The reaction mixture was stirred for 4 h at room temperature, quenched with aqueous $Na_2S_2O_3$ (1.0 M, 30.0 mL), and washed with $H_2O$ (100.0 mL), aqueous $Na_2CO_3$, and brine. The organic layer was dried over $Na_2SO_4$, and the solvent was removed under reduced pressure to give a solid residue. The residue was purified with column chromatography ($SiO_2$, hexane/ethyl acetate = 4:1) to give compound **3** as a white solid (2.96 g, 90%). $^1$H NMR (400 MHz, $CDCl_3$, 298 K): δ = 7.55 (s, 2H), 3.88 (s, 6H), 3.49 (s, 2H), 3.39 (s, 2H), 1.99 (dd, *J* = 9.2, 1.2 Hz, 1H), 1.55 (d, *J* = 9.2 Hz, 1H). $^{13}$C NMR (100 MHz, $CDCl_3$, 298 K): δ = 168.1, 152.0, 130.2, 122.8, 55.6, 52.6, 44.6, 39.3. HRMS (ESI): *m*/*z* calcd for $C_{15}H_{14}O_5Na$ 297.0739 [M + Na]$^+$, found 297.0725.

**Compound 4.** Trimethylaluminum (1.0 M solution in heptane, 1.05 mL, 1.05 mmol) was added to a solution of PhSH (108.0 μL, 1.05 mmol) in dichloromethane (1.5 mL) at 0 °C under nitrogen atmosphere. The reaction mixture was stirred for 20 min, and then the external temperature was lowered to −78 °C. After the temperature stabilized, compound **3** (274 mg, 1.0 mmol) in dichoromethane (1.5 mL) was added and the reaction mixture stirred for another 2 h. The dry ice/acetone bath was taken away, ans the external temperature slowly rose to 298 K. The solution was stirred for an additional 5 h before being quenched with HCl (1.0 M), extracted with dichloromethane (3 × 75 mL), and washed with brine (100 mL). The organic layer was dried with $Na_2SO_4$ and dichloromethane removed under reduced pressure. The solid residue was purified with column chromatography ($SiO_2$, hexane/ethyl acetate = 4:1) to give **4** (276.5 mg, 72%) as a mixture of two diastereomers **4a**$_{rac}$ and **4b**$_{rac}$. The intrinsic instability of this mixture prevented us from separating and/or fully characterizing the two diastereomers. We, however, acquired an $^1$H NMR spectrum of the mixture. $^1$H NMR (400 MHz, $CDCl_3$, 298 K): δ = 7.62−7.22 (m, 14H), 4.04−4.01 (m, 2H), 3.93−3.90 (m, 12H), 3.75 (d, *J* = 12.0 Hz, 1H), 3.49 (s, 2H), 3.42 (m, 2H), 3.37 (s, 1H), 3.19 (d, *J* = 8.0 Hz, 2H), 2.27 (d, *J* = 8.0 Hz, 2H), 2.00 (d, *J* = 8.0 Hz, 2H).

**Compounds 5a$_{rac}$ and 5b$_{rac}$.** A solution of *m*-CPBA (3.68 g, 15.0 mmol) in dichloromethane (80.0 mL) was added to a solution of **4**$_{rac}$ (1.92 g, 5.0 mmol) in dichloromethane (80.0 mL) at 0 °C, and the reaction mixture was stirred for 4 h at room temperature. The reaction was quenched with aqueous $Na_2S_2O_3$ (1.0 M, 50.0 mL), and the organic layer was washed with $H_2O$ (100.0 mL), $Na_2CO_3$ (10%, 200.0 mL), and brine (200.0 mL). The organic solvent was dried over $Na_2SO_4$ and removed under reduced pressure. The residue was purified by flash column chromatography ($SiO_2$, hexane/ethyl acetate = 2:1) to give **5a**$_{rac}$ ($R_f$ = 0.25, 0.64 g) and **5b**$_{rac}$ ($R_f$ = 0.2, 1.4 g) each as a white solid in overall 99% yield. Compound **5b**$_{rac}$. $^1$H NMR (400 MHz, $CDCl_3$, 298 K): δ = 7.97 (d, *J* = 8.0 Hz, 2H), 7.69 (m, 1H), 7.59 (m, 3H), 7.37 (s, 1H), 4.28 (s, 1H), 3.87 (s, 3H), 3.85 (s, 3H), 3.77 (s, 1H), 3.68 (d, *J* = 5.2 Hz, 1H), 3.48 (s, 1H), 3.19 (d, *J* = 6.4 Hz, 1H), 2.75 (d, *J* = 10.4 Hz, 1H), 2.02 (d, *J* = 10.4 Hz, 1H). $^{13}$C NMR (125 MHz, $CDCl_3$, 298 K): δ = 167.9, 167.7, 149.8, 147.9, 139.7, 134.0, 131.2, 131.0, 129.3, 128.4, 123.2, 121.3, 73.8, 67.8, 52.65, 52.64, 51.6, 45.7, 45.2. HRMS (ESI): *m*/*z* calcd for $C_{21}H_{20}O_7SNa$: 439.0827 [M + Na]$^+$, found 439.0822. Compound **5a**$_{rac}$. $^1$H NMR (400 MHz, $CDCl_3$, 298 K): δ = 7.85−7.83 (m, 2H), 7.66−7.52 (m, 3H), 7.46 (s, 2H), 3.83 (s, 1H), 3.80 (s, 3H), 3.79 (s, 3H), 3.77 (s, 1H), 3.42 (t, *J* = 1.6 Hz, 1H), 3.25 (s, 1H), 2.98 (dd, *J* = 6.8, 8.8 Hz, 1H), 2.59 (m, 1H), 1.61 (dd, *J* = 8.8, 12.8 Hz, 1H). $^{13}$C NMR (100 MHz, $CDCl_3$, 298 K): δ = 167.6 (2C), 146.4, 145.5, 137.9, 134.3, 131.3, 130.9, 129.6, 128.1, 123.1, 121.7, 83.2, 66.4, 52.59, 52.57, 49.7, 49.6, 26.8. HRMS (ESI): *m*/*z* calcd for $C_{21}H_{20}O_7SNa$ 439.0827 [M + Na]$^+$, found 439.0812.

**Compounds 6a/6b.** Triethylamine (544 μL, 4.0 mmol), camphanic acid chloride (868 mg, 4.0 mmol), and DMAP (50 mg) were added to a solution of **5** (832 mg, 2.0 mmol) in dry

dichloromethane (44.0 mL) at 0 °C. After the solution was stirred for 2 h at room temperature, a saturated aqueous solution of citric acid was added. The organic layer was washed with $NaHCO_3$ and dried over $Na_2SO_4$. The solvent was removed under reduced pressure and the residue purified by flash column chromatography ($SiO_2$, hexane/ethyl acetate = 2:1) to give diastereomeric **6a** and **6b**, each as a white solid (overall 1.15 g, 96%; approximate 1:1 ratio of **6a**/**6b**). Note that **6a** and **6b** were assigned arbitrarily, and we do not have experimental evidence for distinguishing the two molecules. Each compound was, however, successfully used for completing the synthesis of gated basket **1**. Compound **6a**. $^1$H NMR (400 MHz, $CDCl_3$, 298 K): $\delta$ = 8.00 (d, $J$ = 3.2 Hz, 2H), 7.74−7.61 (m, 4H), 7.20 (s, 1H), 5.51 (dd, $J$ = 6.8, 0.8 Hz, 1H), 3.87 (s, 3H), 3.83 (s, 3H), 3.52 (d, $J$ = 12.8 Hz, 2H), 3.32 (dd, $J$ = 6.8, 1.6, Hz, 1H), 2.86 (d, $J$ = 10.0 Hz, 1H), 2.56 (m, 1H), 2.18 (m, 1H), 2.04 (d, $J$ = 10.0 Hz, 1H), 1.93 (m, 1H), 1.70 (m, 1H), 1.16 (s, 3H), 1.12 (s, 3H), 1.07 (s, 3H). $^{13}$C NMR (100 MHz, $CDCl_3$, 298 K): $\delta$ = 178.3, 167.9, 167.4, 166.5, 149.5, 146.3, 139.7, 134.1, 131.8, 131.0, 129.6, 128.4, 123.8, 121.2, 90.9, 74.3, 66.5, 54.7, 54.3, 52.70, 52.68, 49.7, 46.4, 45.7, 30.7, 28.8, 16.61, 16.58, 9.63. HRMS (ESI): $m/z$ calcd for $C_{31}H_{32}O_{10}SNa$ 619.1614 $[M + Na]^+$, found 619.1605. Compound **6b**. $^1$H NMR (400 MHz, $CDCl_3$, 298 K): $\delta$ = 7.98 (d, $J$ = 3.2 Hz, 2H), 7.74−7.62 (m, 4H), 7.18 (s, 1H), 5.57 (d, $J$ = 7.0 Hz, 1H), 3.87 (s, 3H), 3.85 (s, 3H), 3.48 (d, $J$ = 5.5 Hz, 2H), 3.29 (d, $J$ = 7.0 Hz, 1H), 2.92 (d, $J$ = 8.0 Hz, 1H), 2.87−2.78 (m, 1H), 2.17−2.07 (m, 2H), 2.01−1.93 (m, 1H), 1−76−1.67 (m, 1H), 1.18 (s, 3H), 1.12 (s, 3H), 1.03 (s, 3H). $^{13}$C NMR (100 MHz, $CDCl_3$, 298 K): $\delta$ = 177.8, 167.9, 167.3, 166.3, 149.2, 146.1, 139.8, 134.2, 132.0, 131.1, 129.6, 128.2, 123.9, 121.2, 91.2, 74.3, 66.2, 54.9, 54.3, 52.74, 52.73, 49.9, 46.4, 45.6, 30.7, 29.1, 17.4, 17.0, 9.7. HRMS (ESI): $m/z$ calcd for $C_{31}H_{32}O_{10}SNa$ 619.1614 $[M + Na]^+$, found 619.1605.

**Compounds 7 and 5b.** To a solution of **6a** (1.1 g, 1.8 mmol) in dry $CH_3OH$ (50.0 mL) was added a catalytic amount of $NaOCH_3$/$CH_3OH$ (38.5 mM, 13.0 mL) at 0 °C. The solution was stirred for 5 h at room temperature, the solvent was removed under reduced pressure, and the residue was purified by flash column chromatography ($SiO_2$, hexane/ethyl acetate = 2:1) to give **7** ($R_f$ = 0.3, 82.5 mg, 10%) and **5b** ($R_f$ = 0.25, 640.0 mg, 85%) each as a white solid. Compound **5b**. $^1$H NMR (500 MHz, $CDCl_3$, 298 K): $\delta$ = 7.97 (d, $J$ = 8.0 Hz, 2H), 7.69 (m, 1H), 7.59 (m, 3H), 7.37 (s, 1H), 4.28 (t, $J$ = 6.0 Hz, 1H), 3.87 (s, 3H), 3.85 (s, 3H), 3.77 (s, 1H), 3.68 (d, $J$ = 5.2 Hz, 1H), 3.48 (s, 1H), 3.19 (d, $J$ = 6.4 Hz, 1H), 2.75 (d, $J$ = 10.4 Hz, 1H), 2.02 (d, $J$ = 10.4 Hz, 1H). $^{13}$C NMR (100 MHz, $CDCl_3$, 298 K): $\delta$ = 167.9, 167.7, 149.8, 147.9, 139.7, 134.0, 131.2, 131.0, 129.3, 128.4, 123.2, 121.3, 73.8, 67.8, 52.65, 52.64, 51.6, 45.7, 45.2. HRMS (ESI): $m/z$ calcd for $C_{21}H_{20}O_7SNa$ 439.0827 $[M + Na]^+$, found 439.0822. Compound **7**. $^1$H NMR (400 MHz, $CDCl_3$, 298 K): $\delta$ = 7.90 (m, 2H), 7.68−7.54 (m, 5H), 3.92 (s, 3H), 3.91 (s, 3H), 3.81 (s, 1H), 3.67 (m, 2H), 3.54 (s, 1H), 3.28 (s, 3H), 2.18 (d, $J$ = 5.2 Hz, 1H), 2.05 (d, $J$ = 5.2 Hz, 1H). $^{13}$C NMR (100 MHz, $CDCl_3$, 298 K): $\delta$ = 168.3, 168.0, 146.8, 146.4, 139.5, 133.7, 131.5, 130.4, 129.2, 128.2, 124.8, 122.4, 83.1, 72.7, 57.9, 52.7, 52.6, 49.0, 48.3, 45.3. MS (ESI): $m/z$ calcd for $C_{22}H_{22}O_7SNa$ 453.09 $[M + Na]^+$, found 453.1.

**Compound 8.** To a stirred solution of **5b** (324.5 mg, 0.78 mmol) in anhydrous pyridine (4.0 mL) at 0 °C were added MsCl (179.4 mg, 1.56 mmol) and a catalytic amount of DMAP. The reaction mixture was stirred for 12 h and then quenched with $H_2O$ (20.0 mL). Following, the organic layer was extracted with dichloromethane (50.0 mL), washed with brine (50.0 mL), and dried over $Na_2SO_4$. The organic solvent was removed under reduced pressure and the solid residue purified by column chromatography ($SiO_2$, hexane/ethyl acetate = 2:1) to give mesylate (see the structure above) as a white solid (308.6 mg, 80%). $^1$H NMR (400 MHz, $CDCl_3$, 298 K): $\delta$ = 8.00 (m, 2H), 7.77−7.60 (m, 4H), 7.29 (s, 1H), 5.05 (d, $J$ = 7.2 Hz, 1H), 3.89 (s, 3H), 3.87 (s, 3H), 3.79 (s, 1H), 3.64 (s, 1H), 3.42 (dd, $J$ = 7.2, 1.6 Hz, 1H), 3.16 (s, 3H), 2.75 (d, $J$ = 10.4 Hz, 1H), 2.09 (d, $J$ = 10.4 Hz, 1H). $^{13}$C NMR (100 MHz, $CDCl_3$, 298 K): $\delta$ = 167.8, 167.4, 149.6, 145.7, 139.5, 134.3, 132.0, 131.2, 129.6, 128.6, 124.1, 121.3, 78.8, 66.8, 52.76, 52.74, 50.9, 46.1, 45.3, 38.4. HRMS (ESI): $m/z$ calcd for $C_{22}H_{22}O_9S_2Na$ 517.0603 $[M + Na]^+$, found 517.0618. 1,8-Diazabicycloundec-7-ene (DBU, 253.0 $\mu$L, 1.69 mmol) was slowly added to a solution of mesylate (418.9 mg, 0.847 mmol) in dichloromethane (5.0 mL) at 0 °C, and the reaction mixture was subsequently stirred for 30 min at room temperature. The solvent was removed under reduced pressure and the residue purified by column chromatography ($SiO_2$, hexane/ethyl acetate = 2:1) to give compound **8** as a white solid (303.7 mg, 90%). $^1$H NMR (400 MHz, $CDCl_3$, 298 K): $\delta$ = 7.79−7.43 (m, 7H), 6.92 (s, 1H), 4.19 (s, 1H), 4.06 (s, 1H), 3.87 (s, 3H), 3.85 (s, 3H), 2.61 (d, $J$ = 8.0 Hz, 1H), 2.35 (d, $J$ = 8.0 Hz, 1H). $^{13}$C NMR (100 MHz, $CDCl_3$, 298 K): $\delta$ = 168.0, 167.7, 156.5, 152.5, 151.1, 150.8, 138.3, 133.7, 129.8, 129.44, 129.36, 128.1, 122.5, 122.1, 69.1, 52.7, 52.5, 51.2, 50.6. HRMS (ESI): $m/z$ calcd for $C_{21}H_{18}O_6SNa$ 421.0722 $[M + Na]^+$, found 421.0707.

**Compound 9.** Under an atmosphere of nitrogen, *tert*-butyl isocyanoacetate (184.0 $\mu$L, 1.266 mmol) was added to 1.0 M solution of *t*-BuOK in THF (1.266 mL) at 0 °C. Then, 0.1 M solution of compound **8** (420.0 mg, 1.055 mmol) in dry THF (11.0 mL) was added and the reaction mixture stirred for 4 h at ambient temperature. The reaction was quenched with dilute HCl (5%, 4.5 mL) and the extracted with dichloromethane (25.0 mL). The organic layer was washed with saturated $NaHCO_3$ (25.0 mL) and brine (25.0 mL) and dried over $Na_2SO_4$. The solvent was removed under reduced pressure and the residue was purified by column chromatography ($SiO_2$, hexane/ethyl acetate = 2:1) to give compound **9** as a white solid (365.5 mg, 87%). $^1$H NMR (500 MHz, $CDCl_3$, 298 K): $\delta$ = 8.03 (br, 1H), 7.544 (s, 1H), 7.539 (s, 1H), 6.55 (d, $J$ = 2.5 Hz, 1H), 4.50 (s, 1H), 4.27 (s, 1H), 3.87 (s, 3H), 3.85 (s, 3H), 2.68 (s, 2H), 1.58 (s, 9H). $^{13}$C NMR (100 MHz, $CDCl_3$, 298 K): $\delta$ = 168.5, 168.3, 160.3, 155.2, 154.5, 140.7, 136.0, 129.4, 129.2, 121.7, 121.4, 116.6, 113.3, 80.7, 68.4, 52.5, 52.4, 46.4, 45.6, 28.4. HRMS (ESI): $m/z$ calcd for $C_{22}H_{23}O_6NNa$ 420.1423 $[M + Na]^+$, found 420.1406.

**Compound 10.** Solid iodine (5.4 mg, 0.04 mmol) was added to a solution of **9** (57 mg, 0.143 mmol) in acetonitrile (3.0 mL). Water (30.0 $\mu$L) was added and the reaction mixture refluxed for 5 h. The mixture was then diluted with aqueous $Na_2S_2O_3$ (5.0 mL) and extracted with ethyl acetate (10.0 mL) and the organic layer dried over anhydrous $Na_2SO_4$. The solvent was removed under reduced pressure and the residue purified by column chromatography ($SiO_2$, hexane/ethyl acetate = 1:4) to give carboxylic acid product (see the chemical structure above) as a white solid (35.0 mg, 70%). $^1$H NMR (500 MHz, $CDCl_3$, 298 K): $\delta$ = 8.41 (br, 1H), 7.63 (s, 1H), 7.54 (s, 1H), 6.65 (d, $J$ = 2.5 Hz, 1H), 4.61 (s, 1H), 4.29 (s, 1H), 3.856 (s, 3H), 3.854 (s, 3H), 2.71 (s, 2H). $^{13}$C NMR (125 MHz, $CDCl_3$, 298 K): $\delta$ = 168.4, 168.3, 165.4, 155.1, 154.2, 144.0, 137.1, 129.5, 129.4, 122.2, 121.5, 115.2, 114.4, 68.7, 52.52, 52.50, 46.4, 45.6. HRMS (ESI): $m/z$ calcd for $C_{18}H_{15}O_6NNa$ 364.0797 $[M + Na]^+$, found 364.0782. To a stirred suspension of the carboxylic acid compound (75.0 mg, 0.22 mmol) and benzotriazol-1-yloxytripyrrolidinophosphonium hexafluorophosphate (PyBop) (126 mg, 0.242 mmol) in THF (1.2 mL), *N*,*N*-Diisopropylethylamine (DIPEA) (46 $\mu$L, 0.264 mmol) was added at room temperature. The reaction mixture was allowed to stir for 2 h, the solvent was removed under reduced pressure and the residue was purified by column chromatography ($SiO_2$, hexane/ethyl acetate = 2:1) to give the desired ester (see the chemical structure above) as a white solid (80.0 mg, 80%). $^1$H NMR (500 MHz, $CDCl_3$, 298 K): $\delta$ = 8.90 (br, 1H), 8.06 (d, $J$ = 8.0 Hz, 1H), 7.65 (s, 1H), 7.58 (s, 1H), 7.56−7.39 (m, 3H), 6.84 (d, $J$ = 2.5 Hz, 1H), 4.70 (s, 1H), 4.36 (s, 1H), 3.86 (s, 3H), 3.85 (s, 3H), 2.71 (q, $J$ = 8.0 Hz, 2H). $^{13}$C NMR (125 MHz, $CDCl_3$, 298 K): $\delta$ = 168.3, 168.2, 156.4, 154.8, 153.5, 147.0, 143.5, 138.3, 129.9, 129.6, 129.0, 128.8, 124.9, 122.4, 121.8, 120.4, 118.5, 109.2, 108.6, 69.1, 52.64, 52.63, 47.1, 45.7. HRMS (ESI): $m/z$ calcd for $C_{24}H_{18}O_6N_4Na$ 481.1124 $[M + Na]^+$, found 481.1123. $NaBH_4$ (5.7 mg, 0.15 mmol) was in small portions added to a stirred solution of the Bop ester (46.0 mg, 0.1 mmol) in THF (1 mL) at 0 °C. The reaction mixture was stirred for 2 h at room temperature and the progress of the reduction was followed with TLC ($SiO_2$; $R_f$ = 0.2; hexane/ethyl acetate = 2:1). The reaction mixture was quenched with water (5 mL) and extracted with dichloromethane (3 × 5 mL) and the solvent was removed to give compound **10**. Note that pyrromethanecarbinol **10** is unstable, which prevented us from completing its full characterization. $^1$H NMR (250 MHz, $CDCl_3$, 298 K): $\delta$ = 7.52 (s,


dx.doi.org/10.1021/jo202443j | J. Org. Chem. 2012, 77, 2675−2688

1H), 7.50 (s, 1H), 7.42 (br, 1H), 6.43 (d, $J$ = 2.3 Hz, 1H), 4.59 (s, 1H), 4.57 (s, 1H), 4.25 (s, 2H), 3.857 (s, 3H), 3.852 (s, 3H), 2.62 (q, $J$ = 7.75 Hz, 2H).

**Compound 11.** Pyrromethanecarbinol **10** (19.6 mg, 0.06 mmol) was dissolved in 12 mL of $CHCl_3$, and $p$-TsOH (0.81 mg, 0.00474 mmol) was added to such a mixture at room temperature. After 6 min, DDQ (27.0 mg, 0.12 mmol) was added, and the reaction mixture was stirred for additional 1 h. Upon the addition of triethylamine (12.0 $\mu$L), the reaction mixture was filtered through a pad of alumina and washed with dichloromethane until the eluent was colorless. The solvent was removed under reduced pressure to give crude **11** as a brown solid (5.5 mg, 30%). After an additional purification with preparatory TLC ($SiO_2$, dichloromethane/methanol = 20:1), we obtained octaester **11**. $^1$H NMR (400 MHz, $CDCl_3$, 298 K): $\delta$ = 10.22 (s, 4H), 8.05(s, 8H), 5.81 (s, 8H), 3.77−3.76 (m, 28H), 3.64 (d, $J$ = 7.6 Hz, 4H), −4.83 (s, 2H). $^{13}$C NMR (100 MHz, $CDCl_3$, 27 °C): $\delta$ = 168.2, 155.8, 129.4, 122.6, 101.2, 75.7, 52.4, 49.1. HRMS ESI $m/z$ calcd for $C_{72}H_{53}N_4O_{16}Na$ 1253.3433 $[M + Na]^+$, found 1253.3425.

**Gated Basket 1.** An aqueous solution of LiOH (17 mg of LiOH in 0.7 mL of $H_2O$) was transferred to **11** (12.3 mg, 0.01 mmol) dissolved in THF (0.8 mL), and the reaction mixture was stirred at 80 °C for 3 h. The aqueous phase was acidified with 5% aqueous HCl solution, and the resulting precipitate was filtered, washed with water (2 × 0.5 mL), and dried at 60 °C under high vacuum to give octaacid product (10.1 mg, 90%). $^1$H NMR (500 MHz, MeOD, 298 K): $\delta$ = 11.74 (s, 4H), 8.11 (s, 8H), 6.23 (s, 8H), 3.97 (d, $J$ = 8.0 Hz, 4H), 3.77 (d, $J$ = 8.0 Hz, 4H). $^{13}$C NMR (100 MHz, $CDCl_3$, 298 K): $\delta$ = 169.5, 162.0, 154.3, 130.6, 123.1, 76.4, 49.2. A solution of octaacid (17.0 mg, 0.0152 mmol) in acetic anhydride (1.0 mL) was heated at 130 °C for 2 h. The solvent was removed under high vacuum to give pure tetraanhydride (the chemical structure is shown above) as a brown powder (15.6 mg, 98%). $^1$H NMR (400 MHz, DMSO, 298 K): $\delta$ = 10.68 (s, 4H), 8.24 (s, 8H), 6.14 (s, 8H), 3.89 (d, $J$ = 7.6 Hz, 4H), 3.62 (d, $J$ = 7.6 Hz, 4H), −5.03 (s, 2H). We observed that the tetraanhydride compound would undergo a fast hydrolysis in DMSO, which limited a complete characterization of this compound. Tetraanhydride (15.6 mg, 0.015 mmol) was added to benzylamine (8.0 mg, 0.075 mmol) dissolved in dry DMSO (1.0 mL) and the solution was stirred at room temperature for 2 h. Following, neat pyridine (0.1 mL) was added and the temperature raised to 125 °C. The reaction was allowed to complete (48 h) after which the solvent was evaporated in vacuum and the residue purified by column chromatography ($SiO_2$, dichloromethane/methanol = 20:1) to yield brown solid **1** (10.5 mg, 50%). $^1$H NMR (400 MHz, $CD_2Cl_2$, 298 K): $\delta$ = 10.23 (s, 4H), 7.98 (s, 8H), 7.12−7.04 (m, 20H), 5.87 (s, 8H), 4.52 (s, 8H), 3.88 (d, $J$ = 8.0 Hz, 4H), 3.69 (d, $J$ = 8.0 Hz, 4H), −4.97 (s, 2H). $^{13}$C NMR (125 MHz, $CDCl_3$, 298 K): $\delta$ = 168.0, 159.8, 142.2, 138.8, 136.8, 128.3, 127.9, 127.3, 117.1, 78.2, 49.3, 41.1. HRMS MALDI-TOF: $m/z$ calcd for $C_{92}H_{58}N_8O_8$ 1403.4456 $[M + H]^+$, found 1403.4467.

**Compound Zn(II)−1.** To a solution of basket **1** (2.5 mg, 0.00178 mmol) in $CHCl_3$ (1.5 mL) was added $Zn(OAc)_2{\cdot}2H_2O$ (7.8 mg, 0.036 mmol) in $CH_3OH$ (0.3 mL), upon which the reaction mixture was stirred for 24 h at room temperature. The solvent was removed under reduced pressure and then the residue purified by TLC preparative chromatography ($SiO_2$, dichloromethane/methanol = 15:1) to yield Zn(II)−**1** as a brown solid (1.56 mg, 60%). $^1$H NMR (400 MHz, $CDCl_3$, 298 K): $\delta$ = 10.28 (s, 4H), 8.05 (broad, 8H), 7.23−7.01 (m, 20H), 5.88 (s, 8H), 4.62 (broad, 8H), 3.87 (d, $J$ = 4.0 Hz, 4H), 3.73 (d, $J$ = 4.0 Hz, 4H). MS MALDI-TOF: $m/z$ calcd for $C_{92}H_{56}N_8O_8Zn$ 1464.351 $[M]^+$, found 1464.169. This coordination compound was unstable (MALDI-MS) and fragmented into **1** (see the Supporting Information). The UV−vis spectrum of Zn(II)−**1** is shown in Figure 6B.

Compound Mn(III)−**1**. To a solution of basket **1** (1.5 mg, 0.001 mmol) in $CHCl_3$ (1.0 mL) was added $MnCl_2$ (5.0 mg, 0.04 mmol) in $CH_3OH$ (0.7 mL), and the reaction mixture was stirred for 36 h at room temperature. The solvent was then removed under reduced pressure and the residue purified by TLC preparative chromatography ($SiO_2$, dichloromethane/methanol = 10:1) to yield Mn(III)−**1** as a brown solid (1.2 mg, 80%). HRMS ESI: $m/z$ calcd for $C_{92}H_{57}N_8O_8Mn$ 1456.3680 $[M + H]^+$, found 1456.3628. The UV−vis spectrum of Mn(III)−**1** is shown in Figure 6C.

**1,5-Diadamantylimidazole 14.** Adamantylamine (825.0 mg, 5.46 mmol) and adamantylaldehyde (700.0 mg, 4.27 mmol) were dissolved in benzene (7.0 mL) and refluxed for 4 h with a Dean Stark distilling trap for removing $H_2O$ and forming the Schiff base. Next, benzene was removed under reduced pressure followed by the addition of methanol (7.0 mL) and tosylmethyl isocyanide (819.0 mg, 4.2 mmol). The solution was stirred for 20 h and then heated to reflux for 3 h. The methanol was removed under reduced pressure and the residue extracted with dichloromethane (3 × 50 mL) and brine (50 mL). The organic layer was diluted with hexane to precipitate $p$-toluenesulfonic acid, which was removed by filtration. The dichloromethane solution was concentrated,and the crude product was boiled with an excess of $K_2CO_3$ in 10 mL of methanol for 5 h. The organic solvent was removed under reduced pressure, and the crude product was purified by column chromatography ($SiO_2$, dichloromethane/methanol = 15:1) to give **14** as a white solid (366.9 mg, 20%). $^1$H NMR (500 MHz, $CDCl_3$, 298 K): $\delta$ = 7.80 (s, 1H), 7.02 (s, 1H), 2.35 (d, $J$ = 2.5 Hz, 6H), 2.29 (s, 3H), 2.16 (d, $J$ = 2.5 Hz, 6H), 2.12 (s, 3H), 1.78 (m, 12H); $^{13}$C NMR (125 MHz, $CDCl_3$, 298 K): $\delta$ = 143.8, 136.3, 125.6, 70.6, 61.2, 43.9, 43.4, 36.4, 35.6, 30.1, 28.7 ppm; HRMS (ESI): $m/z$ calcd for $C_{23}H_{32}N_2$ 337.2644 $[M + H]^+$, found 337.2633.

## ■ ASSOCIATED CONTENT

### Supporting Information

Detailed description of $^1$H NMR and UV−vis spectroscopic titration experiments and the epoxidation procedures. This material is available free of charge via the Internet at http://pubs.acs.org.

## ■ AUTHOR INFORMATION


### Corresponding Author

*Tel: 614 247 8342. Fax: 614 292 1685. E-mail: badjic@chemistry.ohio-state.edu.


### Notes

The authors declare no competing financial interest.

## ■ ACKNOWLEDGMENTS


This work was financially supported with funds obtained from the National Science Foundation under CHE-1012146 by the Department of the Defense, Defense Threat Reduction Agency (HDTRA1-11-1-0042). The content of the information does not necessarily reflect the position or the policy of the federal government, and no official endorsement should be inferred. We thank the Ohio Supercomputer Center for generous computational resources.


## ■ REFERENCES


(1) Cram, D. J. *Science (Washington, DC, U.S.)* **1983**, *219*, 1177.
(2) MacGillivray, L. R.; Atwood, J. L. *Angew. Chem., Int. Ed.* **1999**, *38*, 1018.
(3) Jasat, A.; Sherman, J. C. *Chem. Rev. (Washington, DC, U.S.)* **1999**, *99*, 931.
(4) Brotin, T.; Dutasta, J.-P. *Chem. Rev. (Washington, DC, U.S.)* **2009**, *109*, 88.
(5) Hof, F.; Craig, S. L.; Nuckolls, C.; Rebek, J. Jr. *Angew. Chem., Int. Ed.* **2002**, *41*, 1488.
(6) Yeh, R. M.; Davis, A. V.; Raymond, K. N. *Compr. Coord. Chem. II* **2004**, *7*, 327.
(7) Badjic, J. D.; Stojanovic, S.; Ruan, Y. *Adv. Phys. Org. Chem.* **2011**, *45*, 1.
(8) Sherman, J. C.; Cram, D. J. *J. Am. Chem. Soc.* **1989**, *111*, 4527.
(9) Warmuth, R.; Makowiec, S. *J. Am. Chem. Soc.* **2007**, *129*, 1233.
(10) Warmuth, R. *Eur. J. Org. Chem.* **2001**, 423.

(11) Yoshizawa, M.; Klosterman, J. K.; Fujita, M. *Angew. Chem., Int. Ed.* **2009**, *48*, 3418.
(12) Wiester, M. J.; Ulmann, P. A.; Mirkin, C. A. *Angew. Chem., Int. Ed.* **2011**, *50*, 114.
(13) Hu, S.; Li, J.; Xiang, J.; Pan, J.; Luo, S.; Cheng, J.-P. *J. Am. Chem. Soc.* **2010**, *132*, 7216.
(14) Bao, X.; Rieth, S.; Stojanovic, S.; Hadad, C. M.; Badjic, J. D. *Angew. Chem., Int. Ed.* **2010**, *49*, 4816.
(15) Rieth, S.; Hermann, K.; Wang, B.-Y.; Badjic, J. D. *Chem. Soc. Rev.* **2011**, *40*, 1609.
(16) Houk, K. N.; Nakamura, K.; Sheu, C.; Keating, A. E. *Science (Washington, DC, U.S.)* **1996**, *273*, 627.
(17) Quan, M. L. C.; Cram, D. J. *J. Am. Chem. Soc.* **1991**, *113*, 2754.
(18) Zhou, H.-X.; Wlodek, S. T.; McCammon, J. A. *Proc. Natl. Acad. Sci. U.S.A.* **1998**, *95*, 9280.
(19) Zhou, H.-X.; McCammon, J. A. *Trends Biochem. Sci.* **2010**, *35*, 179.
(20) Menger, F. M. *Acc. Chem. Res.* **1985**, *18*, 128.
(21) Menger, F. M. *Pure Appl. Chem.* **2005**, *77*, 1873.
(22) Wang, B.-Y.; Bao, X.; Yan, Z.; Maslak, V.; Hadad, C. M.; Badjic, J. D. *J. Am. Chem. Soc.* **2008**, *130*, 15127.
(23) Rieth, S.; Bao, X.; Wang, B.-Y.; Hadad, C. M.; Badjic, J. D. *J. Am. Chem. Soc.* **2010**, *132*, 773.
(24) Rieth, S.; Badjic, J. D. *Chem.—Eur. J.* **2011**, *17*, 2562.
(25) Wang, B.-Y.; Rieth, S.; Badjic, J. D. *J. Am. Chem. Soc.* **2009**, *131*, 7250.
(26) Maslak, V.; Yan, Z.; Xia, S.; Gallucci, J.; Hadad, C. M.; Badjic, J. D. *J. Am. Chem. Soc.* **2006**, *128*, 5887.
(27) Wang, X.; Houk, K. N. *Org. Lett.* **1999**, *1*, 591.
(28) Raymo, F. M.; Houk, K. N.; Stoddart, J. F. *J. Am. Chem. Soc.* **1998**, *120*, 9318.
(29) Sheu, C.; Houk, K. N. *J. Am. Chem. Soc.* **1996**, *118*, 8056.
(30) Palmer, L. C.; Rebek, J. Jr. *Org. Biomol. Chem.* **2004**, *2*, 3051.
(31) Hooley, R. J.; Van Anda, H. J.; Rebek, J. Jr. *J. Am. Chem. Soc.* **2006**, *128*, 3894.
(32) Helgeson, R. C.; Hayden, A. E.; Houk, K. N. *J. Org. Chem.* **2010**, *75*, 570.
(33) Wang, J.; Feringa, B. L. *Science (Washington, DC, U.S.)* **2011**, *331*, 1429.
(34) Davis, A. V.; Yeh, R. M.; Raymond, K. N. *Proc. Natl. Acad. Sci. U.S.A.* **2002**, *99*, 4793.
(35) Wu, B.; Parquette, J. R.; RajanBabu, T. V. *Science (Washington, DC, U.S.)* **2009**, *326*, 1662.
(36) Liu, S.; Gan, H.; Hermann, A. T.; Rick, S. W.; Gibb, B. C. *Nat. Chem.* **2010**, *2*, 847.
(37) Ramondenc, Y.; Schwenninger, R.; Phan, T.; Gruber, K.; Kratky, C.; Kraeulter, B. *Angew. Chem.* **1994**, *106*, 939.
(38) Mecozzi, S.; Rebek, J. Jr. *Chem.—Eur. J.* **1998**, *4*, 1016.
(39) Wang, B.-Y.; Turner, D. A.; Zujovic, T.; Hadad, C. M.; Badjic, J. D. *Chem.—Eur. J.* **2011**, *17*, 8870.
(40) McLain, J. L.; Lee, J.; Groves, J. T. *Biomimetic Oxid. Catal. Transition Met. Complexes* **2000**, 91.
(41) Meunier, B.; de Visser, S. P.; Shaik, S. *Chem. Rev. (Washington, DC, U.S.)* **2004**, *104*, 3947.
(42) Meunier, B.; Robert, A.; Pratviel, G.; Bernadou, J. *Porphyrin Handbook* **2000**, *4*, 119.
(43) Feiters, M. C.; Rowan, A. E.; Nolte, R. J. M. *Chem. Soc. Rev.* **2000**, *29*, 375.
(44) Collman, J. P.; Zhang, X.; Lee, V. J.; Uffelman, E. S.; Brauman, J. I. *Science (Washington, DC, U.S.)* **1993**, *261*, 1404.
(45) Macikenas, D.; Skrzypczak-Jankun, E.; Protasiewicz, J. D. *J. Am. Chem. Soc.* **1999**, *121*, 7164.
(46) Meprathu, B. V.; Protasiewicz, J. D. *Tetrahedron* **2010**, *66*, 5768.
(47) Song, W. J.; Seo, M. S.; DeBeer George, S.; Ohta, T.; Song, R.; Kang, M.-J.; Tosha, T.; Kitagawa, T.; Solomon, E. I.; Nam, W. *J. Am. Chem. Soc.* **2007**, *129*, 1268.
(48) Zhang, R.; Horner, J. H.; Newcomb, M. *J. Am. Chem. Soc.* **2005**, *127*, 6573.
(49) Groves, J. T.; Lee, J.; Marla, S. S. *J. Am. Chem. Soc.* **1997**, *119*, 6269.
(50) Rieth, S.; Yan, Z.; Xia, S.; Gardlik, M.; Chow, A.; Fraenkel, G.; Hadad, C. M.; Badjic, J. D. *J. Org. Chem.* **2008**, *73*, 5100.
(51) Panigot, M. J.; Waters, J. F.; Varde, U.; Sutter, J. K.; Sukenik, C. N. *Macromolecules* **1992**, *25*, 530.
(52) See the Supporting Information.
(53) Liu, C.; Hashimoto, Y.; Kudo, K.; Saigo, K. *Bull. Chem. Soc. Jpn.* **1996**, *69*, 2095.
(54) Moreno-Vargas Antonio, J.; Schutz, C.; Scopelliti, R.; Vogel, P. *J. Org. Chem.* **2003**, *68*, 5632.
(55) Shelnutt, J. A.; Song, X.-Z.; Ma, J.-G.; Jia, S.-L.; Jentzen, W.; Medforth, C. J. *Chem. Soc. Rev.* **1998**, *27*, 31.
(56) Haddad, R. E.; Gazeau, S.; Pecaut, J.; Marchon, J.-C.; Medforth, C. J.; Shelnutt, J. A. *J. Am. Chem. Soc.* **2003**, *125*, 1253.
(57) Ito, S.; Murashima, T.; Ono, N.; Uno, H. *Chem. Commun. (Cambridge)* **1999**, 2275.
(58) Barkigia, K. M.; Berber, M. D.; Fajer, J.; Medforth, C. J.; Renner, M. W.; Smith, K. M. *J. Am. Chem. Soc.* **1990**, *112*, 8851.
(59) Somma, M. S.; Medforth, C. J.; Nelson, N. Y.; Olmstead, M. M.; Khoury, R. G.; Smith, K. M. *Chem. Commun. (Cambridge)* **1999**, 1221.
(60) Lu, H.; Zhang, X. P. *Chem. Soc. Rev.* **2011**, *40*, 1899.
(61) Collman, J. P.; Zhang, X.; Hembre, R. T.; Brauman, J. I. *J. Am. Chem. Soc.* **1990**, *112*, 5356.
(62) Collman, J. P.; Kodadek, T.; Raybuck, S. A.; Meunier, B. *Proc. Natl. Acad. Sci. U.S.A.* **1983**, *80*, 7039.
(63) Ogoshi, H.; Mizutani, T.; Hayashi, T.; Kuroda, Y. *Porphyrin Handbook* **2000**, *6*, 279.
(64) Middel, O.; Verboom, W.; Reinhoudt, D. N. *J. Org. Chem.* **2001**, *66*, 3998.
(65) Ahlrichs, R.; Baer, M.; Haeser, M.; Horn, H.; Koelmel, C. *Chem. Phys. Lett.* **1989**, *162*, 165.
(66) Eichkorn, K.; Weigend, F.; Treutler, O.; Ahlrichs, R. *Theor. Chem. Acc.* **1997**, *97*, 119.
(67) Haeser, M.; Ahlrichs, R. *J. Comput. Chem.* **1989**, *10*, 104.
(68) Von Arnim, M.; Ahlrichs, R. *J. Comput. Chem.* **1998**, *19*, 1746.
(69) La Mar, G. N.; Walker, F. A. *J. Am. Chem. Soc.* **1975**, *97*, 5103.
(70) de Sousa, A. N.; de Carvalho, M. E. M. D.; Idemori, Y. M. *J. Mol. Catal. A Chem.* **2001**, *169*, 1.
(71) Kirner, J. F.; Reed, C. A.; Scheidt, W. R. *J. Am. Chem. Soc.* **1977**, *99*, 2557.
(72) Kirner, J. F.; Reed, C. H.; Scheidt, W. R. J *Am Chem Soc* **1977**, *99*, 2557.
(73) Kirner, J. F.; Scheidt, W. R. *Inorg. Chem.* **1975**, *14*, 2081.
(74) Ballester, P.; Costa, A.; Castilla, A. M.; Deya, P. M.; Frontera, A.; Gomila, R. M.; Hunter, C. A. *Chem.—Eur. J.* **2005**, *11*, 2196.
(75) Ballester, P.; Costa, A.; Deya, P. M.; Frontera, A.; Gomila, R. M.; Oliva, A. I.; Sanders, J. K. M.; Hunter, C. A. *J. Org. Chem.* **2005**, *70*, 6616.
(76) Hirose, K. *Anal. Methods Supramol. Chem.* **2007**, 17.
(77) Thordarson, P. *Chem. Soc. Rev.* **2011**, *40*, 1305.
(78) Ercolani, G.; Schiaffino, L. *Angew. Chem., Int. Ed.* **2011**, *50*, 1762.
(79) Ercolani, G. *J. Am. Chem. Soc.* **2003**, *125*, 16097.
(80) Yuan, L. C.; Bruice, T. C. *J. Am. Chem. Soc.* **1986**, *108*, 1643.
(81) Park, S.-E.; Song, W. J.; Ryu, Y. O.; Lim, M. H.; Song, R.; Kim, K. M.; Nam, W. *J. Inorg. Biochem.* **2005**, *99*, 424.
(82) Elemans, J. A. A. W.; Bijsterveld, E. J. A.; Rowan, A. E.; Nolte, R. J. M. *Eur. J. Org. Chem.* **2007**, 751.
(83) Crestoni, M. E.; Fornarini, S.; Lanucara, F. *Chem.—Eur. J.* **2009**, *15*, 7863.
(84) Collman, J. P.; Brauman, J. I.; Fitzgerald, J. P.; Hampton, P. D.; Naruta, Y.; Michida, T. *Bull. Chem. Soc. Jpn.* **1988**, *61*, 47.
(85) Harmer, H. R.; Reimer, K. J.; Smith, D. W.; James, B. R. *Inorg. Chim. Acta* **1989**, *166*, 167.
(86) Fiedler, D.; Leung, D. H.; Bergman, R. G.; Raymond, K. N. *Acc. Chem. Res.* **2005**, *38*, 349.
(87) Breiner, B.; Clegg, J. K.; Nitschke, J. R. *Chem. Sci.* **2011**, *2*, 51.

(88) Pluth, M. D.; Bergman, R. G.; Raymond, K. N. *Acc. Chem. Res.* **2009**, *42*, 1650.
(89) Nishioka, Y.; Yamaguchi, T.; Yoshizawa, M.; Fujita, M. *J. Am. Chem. Soc.* **2007**, *129*, 7000.
(90) Yoshizawa, M.; Tamura, M.; Fujita, M. *Science (Washington, DC, U.S.)* **2006**, *312*, 1472.
(91) Sundaresan, A. K.; Ramamurthy, V. *Org. Lett.* **2007**, *9*, 3575.
(92) Thordarson, P.; Bijsterveld, E. J. A.; Rowan, A. E.; Nolte, R. J. M. *Nature (London, U.K.)* **2003**, *424*, 915.
(93) Collman, J. P.; Zhang, Z.; Lee, V.; Hembre, R. T.; Brauman, J. I. *Adv. Chem. Ser.* **1992**, *230*, 153.
(94) Elemans, J. A. A. W.; Bijsterveld, E. J. A.; Rowan, A. E.; Nolte, R. J. M. *Chem. Commun. (Cambridge)* **2000**, 2443.
(95) Collman, J. P.; Zeng, L.; Wang, H. J. H.; Lei, A.; Brauman, J. I. *Eur. J. Org. Chem.* **2006**, 2707.
(96) Bhyrappa, P.; Young, J. K.; Moore, J. S.; Suslick, K. S. *J. Mol. Catal. A Chem.* **1996**, *113*, 109.
(97) Hull, J. F.; Sauer, E. L. O.; Incarvito, C. D.; Faller, J. W.; Brudvig, G. W.; Crabtree, R. H. *Inorg. Chem. (Washington, DC, U.S.)* **2009**, *48*, 488.
(98) Lai, T.-S.; Lee, S. K. S.; Yeung, L.-L.; Liu, H.-Y.; Williams, I. D.; Chang, C. K. *Chem. Commun. (Cambridge, U.K.)* **2003**, 620.
(99) Suslick, K. S. *Porphyrin Handbook* **2000**, *4*, 41.
(100) Groves, J. T.; Nemo, T. E. *J. Am. Chem. Soc.* **1983**, *105*, 5786.
(101) Suslick, K. S.; Cook, B. R. *J. Chem. Soc., Chem. Commun.* **1987**, 200.
(102) Schardt, B. C.; Smegal, J. A.; Hollander, F. J.; Hill, C. L. *J. Am. Chem. Soc.* **1982**, *104*, 3964.
(103) Meunier, B.; Guilmet, E.; De Carvalho, M. E.; Poilblanc, R. *J. Am. Chem. Soc.* **1984**, *106*, 6668.
(104) Battioni, P.; Renaud, J. P.; Bartoli, J. F.; Reina-Artiles, M.; Fort, M.; Mansuy, D. *J. Am. Chem. Soc.* **1988**, *110*, 8462.
(105) Collman, J. P.; Brauman, J. I.; Hampton, P. D.; Tanaka, H.; Bohle, D. S.; Hembre, R. T. *J. Am. Chem. Soc.* **1990**, *112*, 7980.
(106) Collman, J. P.; Brauman, J. I.; Meunier, B.; Raybuck, S. A.; Kodadek, T. *Proc. Natl. Acad. Sci. U.S.A.* **1984**, *81*, 3245.
(107) Van der Made, A. W.; Nolte, R. J. M. *J. Mol. Catal.* **1984**, *26*, 333.
(108) Vedejs, E.; Jure, M. *Angew. Chem., Int. Ed.* **2005**, *44*, 3974.
(109) Bhyrappa, P.; Young, J. K.; Moore, J. S.; Suslick, K. S. *J. Am. Chem. Soc.* **1996**, *118*, 5708.